PLoS GENETICS

The Recombinases Rad51 and Dmc1 Play Distinct Roles in DNA Break Repair and Recombination Partner Choice in the Meiosis of *Tetrahymena*

Rachel A. Howard-Till, Agnieszka Lukaszewicz, Josef Loidl*

Department of Chromosome Biology and Max F. Perutz Laboratories, Center for Molecular Biology, University of Vienna, Vienna, Austria

Abstract

Repair of programmed DNA double-strand breaks (DSBs) by meiotic recombination relies on the generation of flanking 3′ single-stranded DNA overhangs and their interaction with a homologous double-stranded DNA template. In various common model organisms, the ubiquitous strand exchange protein Rad51 and its meiosis-specific homologue Dmc1 have been implicated in the joint promotion of DNA–strand exchange at meiotic recombination sites. However, the division of labor between these two recombinases is still a puzzle. Using RNAi and gene-disruption experiments, we have studied their roles in meiotic recombination and chromosome pairing in the ciliated protist *Tetrahymena* as an evolutionarily distant meiotic model. Cytological and electrophoresis-based assays for DSBs revealed that, without Rad51p, DSBs were not repaired. However, in the absence of Dmc1p, efficient Rad51p-dependent repair took place, but crossing over was suppressed. Immunostaining and protein tagging demonstrated that only Dmc1p formed strong DSB–dependent foci on meiotic chromatin, whereas the distribution of Rad51p was diffuse within nuclei. This suggests that meiotic nucleoprotein filaments consist primarily of Dmc1p. Moreover, a proximity ligation assay confirmed that little if any Rad51p forms mixed nucleoprotein filaments with Dmc1p. Dmc1p focus formation was independent of the presence of Rad51p. The absence of Dmc1p did not result in compensatory assembly of Rad51p repair foci, and even artificial DNA damage by UV failed to induce Rad51p foci in meiotic nuclei, while it did so in somatic nuclei within one and the same cell. The observed interhomologue repair deficit in *dmc1Δ* meiosis is consistent with a requirement for Dmc1p in promoting the homologue as the preferred recombination partner. We propose that relatively short and/or transient Rad51p nucleoprotein filaments are sufficient for intrachromosomal recombination, whereas long nucleoprotein filaments consisting primarily of Dmc1p are required for interhomolog recombination.

Introduction

Meiosis is a pivotal process in the sexual reproduction cycle. It is a nuclear division that reduces the diploid somatic to the haploid gametic chromosome set. Successful disjunction of the two genomes requires that every chromosome pairs with its corresponding partner before they eventually separate. In most organisms, chromosome pairing relies on the base pair matching of single-stranded DNA molecules that are generated in the wake of self-inflicted DNA double-strand breaks (DSBs). Repair of DSBs occurs by using an intact DNA strand as a template, and may lead to the exchange of the broken and the template strand, thereby causing meiotic genetic recombination. It is essential that DNA from the homologous chromosome is preferred as a template for recombinational repair over DNA from the sister chromatid, since only the former situation will generate crossovers that ensure the orderly segregation of homologous chromosomes during the reductional division.

Strand exchange at meiotic recombination sites is accomplished by the RecA homologs Rad51 and Dmc1. They have similar and partially overlapping roles in DNA heteroduplex formation [1], but whereas Rad51 is indispensable both for mitotic and meiotic recombination, Dmc1 is meiosis-specific. It has been suggested that this is due to its role in interhomolog rather than intersister recombination [2]. Consequently, in budding yeast, where Rad51-dependent repair via the sister is suppressed in meiosis (see [3] and lit cit. therein), meiotic DSB repair is dramatically reduced and DSBs acquire long single-stranded tails in the absence of Dmc1 [4]. However, upon overexpression of Rad51 or its stimulating partner Rad54, and in certain mutant strains, high levels of interhomolog recombination can occur in the absence of Dmc1 [5–7]. Thus, it seems that Rad51 is not, in principle, unable to support interhomolog recombination, but that it is held in check during meiosis. It may be impeded in order to promote a Dmc1-dependent pathway, which may perform better in meiotic crossover, especially in recombination partner choice. Dmc1 is also required for interhomolog recombination in mammals [8,9]. In other organisms, this division of labor is not as strict, and the *dmc1* mutant phenotype is less severe. In *Arabidopsis dmc1* mutants, chromosome fragmentation was not observed, and chromosomes segregated randomly at meiosis I. This indicated that DSBs were repaired by a mechanism that did not produce crossovers [10,11].

Author Summary

Sexual reproduction relies on meiosis, the specialized cell division that allows diploid organisms to halve their chromosome content, resulting in the production of gametes containing one copy of each chromosome. In humans, defects in meiosis cause infertility, stillbirths, and congenital diseases. Homologous recombination is a key step in the meiotic program and is essential for maintaining the fidelity of segregation and for creating genetic diversity. Meiotic recombination begins with self-inflicted DNA breaks that are repaired using the homologous chromosome as a template, in a process that depends upon the universal repair protein Rad51 and its meiosis-specific homologue, Dmc1. The relative contributions of Rad51 and Dmc1 to homologous recombination differ among yeasts, plants, and mammals. We have undertaken a study of these proteins in the evolutionarily distant model organism *Tetrahymena thermophila* with the hope of clarifying the specialization of these recombinases throughout eukaryotic evolution. We show that, while Rad51 is required for DNA repair, only Dmc1 localizes prominently to meiotic DNA break sites. Also, repair via the homologous chromosome depends on Dmc1. These results suggest that nucleoprotein filaments consisting of primarily Dmc1p allow efficient interhomologue repair, while shorter Rad51 filaments may suffice for repair via the sister chromatid.

In the fission yeast, *Schizosaccharomyces pombe*, deletion of *DMC1* caused only a moderate reduction in crossing over and a slight reduction in fertility, suggesting that Rad51 can partially substitute for Dmc1 in interhomolog recombination [12]. *Drosophila*, *Caenorhabditis elegans*, and *Neurospora* lack Dmc1 orthologues, altogether (see [1]).

Because of the variability between model organisms with respect to their dependence on Rad51 and Dmc1 for meiotic crossing over, we decided to study the roles of Rad51p and Dmc1p in the unconventional meiosis of the evolutionarily distant model system *Tetrahymena*. *Tetrahymena thermophila* is a unicellular ciliated protist that possesses two nuclei, the polyploid somatic macronucleus and the diploid generative micronucleus. While the former is transcriptionally active and divides by an amitotic process, the latter constitutes the germline, is transcriptionally silent, and divides mitotically. Only the micronucleus undergoes meiosis. Both the rough alignment and the precise matching of homologous chromosomes during meiotic prophase depend on Spo11-induced meiotic DSBs and their signaling through an ATR-dependent pathway [13].

Promotion of Dmc1 over Rad51 usage in meiosis seems to be, in part, related to the presence of a synaptonemal complex (SC) (see [7] and lit cit. therein), and *Tetrahymena* does not feature a canonical SC. Therefore, we wondered whether dependency on Dmc1 would be low. To test this, we designed experiments to elucidate the contributions of Rad51 and Dmc1 to meiotic recombination in *Tetrahymena*.

Results

Rad51p and Dmc1p show different expression patterns, and depletion of either has different effects on fertility

The differing importance of *RAD51* and *DMC1* for meiosis in a variety of organisms led us to study in detail, the role of these two genes in the meiosis of the protist *Tetrahymena*. The situation in this evolutionarily distant model system may help to clarify the

primordial division of labor between the two proteins. *Tetrahymena* possesses two RecA homologs, TTHERM_00142330 (*RAD51*) and TTHERM_00459230 (*DMC1*) [14]. *RAD51* is expressed during the mitotic cell cycle with a particularly high abundance of *RAD51* mRNA during S phase of the somatic nucleus, and during meiotic prophase [15]. It is also strongly induced following DNA damage [16,17]. Consistent with its somatic expression pattern, it has been reported that Rad51p is essential for vegetative growth [15]. Also, small amounts of Rad51p were found in the somatic nucleus ([18] and Figure S1A). *DMC1*, on the other hand, showed meiosis-specific expression in mRNA microarray hybridizations
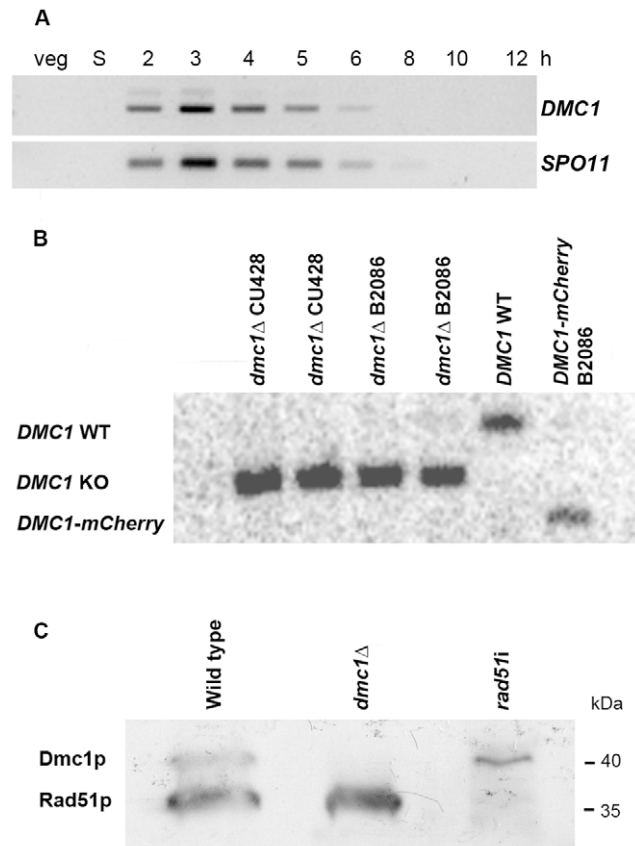

Figure 1. Expression of Dmc1p and Rad51p. (A) Expression pattern of *DMC1* as visualized by RT-PCR. While there is no transcription in vegetatively (veg) growing and starving (S) cells, *DMC1* mRNA is maximally abundant in early meiotic cells from 2–4 h after meiosis induction. Timing of expression is the same as that of *SPO11*. (B) Southern hybridization with a probe adjacent to the 3′end of the *DMC1* locus. Digestion of genomic DNA from knockout, wild-type and *DMC1-mCherry* strains with EcoRI, which differentially cuts internally in the knockout and tagging constructs, produced the detected fragments of 2.1 kb, 2.8 kb, and 1.8 kb, respectively. The absence of the 2.8 kb fragment in knockout samples indicates that the replacement of the expressed wild-type sequences in the somatic nucleus by the knockout cassette is complete in several lines of both mating types. Also shown is the complete replacement of wild-type *DMC1* by a version fused to a sequence encoding the mCherry fluorescent marker. (C) Western detection of Rad51p and Dmc1p with an antibody that recognizes both proteins. At t = 3.5 h after meiosis induction, both Rad51p and Dmc1p are expressed in wild type conjugating cells. In the *dmc1Δ* strain, no detectable amount of Dmc1p was expressed 3.5 h after meiosis induction. In a crossing of two *rad51*i strains, expression of Rad51p was strongly reduced. Positions of 35 kDa and 40 kDa marker bands are indicated.

doi:10.1371/journal.pgen.1001359.g001

[19]. Here, we confirmed the exclusive meiotic expression by RT-PCR and showed that maximal expression occurs approximately 3 h after induction of meiosis, which is similar to that of *SPO11* (Figure 1A).

To investigate the functions of Rad51p and Dmc1p, we produced strains lacking one or the other. *dmc1*Δ strains were constructed by knocking out the ~45 transcriptionally active copies of *DMC1* in the polyploid somatic nucleus by gene replacement. Southern hybridization demonstrated the removal of the wild-type copies (Figure 1B), and the complete lack of Dmc1p was confirmed by Western detection (Figure 1C). The requirement of Rad51p for vegetative growth precluded gene knockout. Therefore, we created a strain carrying a *RAD51* hairpin construct (*rad51*hp), which expressed double-stranded RNA hairpins under a Cd^{2+}-inducible promoter [20]. This allowed the knockdown of *RAD51* by RNA interference (RNAi) specifically during meiosis. High efficiency of RNAi was confirmed by Western analysis (Figure 1C), where the protein was estimated to be reduced to ~1% of the wild-type level (Figure S1). Also, *rad51* knockdown (*rad51*i) cells were unable to express Rad51p upon UV-induced DNA-damage (Figure S1). We triggered RNAi by the exposure of cells to $CdCl_2$ in stationary cultures before the initiation of meiosis (see Materials and Methods). This regime avoids depletion of Rad51p needed for vegetative propagation, yet allows for abundant hairpin expression to knock down *RAD51* during meiosis.

First, we tested the ability of Rad51p- and Dmc1p-depleted cells to undergo meiosis and sexual reproduction (Table 1; explanations in Table 1). While *rad51*i cells did not produce any sexual progeny, the viability of sexual progeny from *dmc1* KO crosses was found to be 3.4% (as compared to 98% of wild-type crosses - Table 1). Thus, a low proportion of *dmc1*Δ meioses can give rise to viable zygotes.

Table 1. Meiosis success as indicated by the production of sexual progeny.

Matings [1]	n	% of matings producing viable descendants [2]	% of matings producing sexual progeny [2]
WT × WT	88	99	**98**
*rad51*hp × *rad51*hp [3]	88	90	**60**
*rad51*i × *rad51*i [3]	88	55	**0**
*dmc1*Δ × *dmc1*Δ	88	59	**3.4**
DMC1-mCherry × *dmc1*Δ	88	53	**25**

n = number of conjugating (mating) pairs tested.
1 In *Tetrahymena*, conjugating cells produce sexual progeny by exchanging haploid meiotic products, whereupon both partners form zygotes. These mature into four genetically uniform karyonides which then begin vegetative multiplication by binary fission (e.g., [55,56]). Success of meiosis was quantified by determining the percentage of conjugating pairs (matings) that produced viable sexual progeny.
2 If meiosis is faulty, matings may fail to produce progeny altogether or cells return to vegetative growth and produce clonal descendants. Thus viable descendants must be tested for their origin from successful meiosis. Clonal descendants possess the old somatic nucleus, which, in the parental strains, express a paromomycin resistance gene. Clonal descendants are therefore paromomycin-resistant. During sexual reproduction, the old somatic nuclei are degraded and new somatic nuclei lack the resistance gene, therefore sexual progeny are characterized by their paromomycin-sensitivity.
3 *rad51*hp cells carry the RNAi hairpin construct but are not transcribing the hairpin RNA, whereas in *rad51*i cells hairpin transcription, and hence RNAi, is induced by treatment with $CdCl_2$ (see Materials and methods).
doi:10.1371/journal.pgen.1001359.t001

Meiotic progression and DSB repair are inhibited in the absence of Rad51p

To determine the basis of the different meiotic success rates of Rad51- and Dmc1-depleted cells, we studied meiotic progression cytologically in *rad51*i and *dmc1*Δ strains.

In *Tetrahymena*, nutrient-starvation makes cells competent for conjugation (= cell mating). Upon mixing starved cells of complementing mating types, they will form pairs which initiate synchronous meioses of their generative nuclei (see [21,22]). Meiotic prophase is characterized by an enormous elongation of the nuclei (Figure 2A). The appearance of DSBs and increasing chromosome pairing during the elongation process permit the attribution of the elongating meiotic nucleus to the leptotene-pachytene stages (see [13]). During a stage corresponding to diplotene, the nucleus shortens again and chromosomes condense. Five bivalents emerge in diakinesis-metaphase I and finally undergo two meiotic divisions (Figure 2A).

It was previously found in a *rad51* knockout strain that meiotic nuclei did elongate, but that cells arrested prior to chromosome condensation and rarely progressed to anaphase I [15]. However, due to the vegetative function of Rad51p, the observed phenotypes could have been caused by accumulative pre-meiotic damage rather than genuine meiotic defects [15]. To prevent mitotic defects from obscuring the meiotic phenotype of Rad51p loss, we induced RNAi knockdown of *RAD51* only at the onset of meiosis [20].

Cytological inspection of conjugating RNAi cells (*rad51*i) revealed that stages up to diplotene were indistinguishable from wild-type (Figure 2B). However, diakinesis-metaphase I showed signs of chromosome fragmentation (Figure 2B, 3A) with 98% of the nuclei at that stage (n = 100) displaying granular or diffuse chromatin and only 2% featuring compact entities. Moreover, normal meiotic divisions did not take place (Figure 2B). In a similar experiment, a *rad51*i strain was conjugated to a wild-type strain. In this case, both partners were affected due to the trans-activity of RNAi (see Materials and Methods). As a control, a *rad51*hp strain without stimulation of RNAi was mated to a wild type strain, confirming that the mere presence of the construct did not notably interfere with the progress of meiosis (Figure S2). Thus, the fragmentation of metaphase I chromosomes and the inability to perform normal meiotic divisions upon induced RNAi are genuine consequences of the depletion of Rad51p and not side-effects of the experimental system.

The fragmented metaphase I chromosomes strongly indicated that DSBs were not properly repaired. To confirm the persistence of DSBs, we performed an assay for the detection of DSB-dependent chromosome fragmentation by pulsed-field gel electrophoresis (PFGE) [13]. Under our standard PFGE conditions, intact chromosomes of the generative nucleus do not enter the gel, whereas DNA fragments of different size migrate as a distinct band [13]. In the wild type, DSB-dependent fragments appeared from ~2 h–5 h after induction of meiosis (Figure 3B). They were missing in a *spo11*Δ strain, which is unable to generate meiotic DSBs (Figure 3B). In *rad51*i meiosis, the band diagnostic for DSBs did not disappear within 6 h from induction of meiosis (Figure 3B). Thus, meiotic DSBs are not repaired in the absence of Rad51p (Figure 3B). However, in repeated experiments this band consistently became weaker at 6 h post-meiosis induction. We speculate that this reduction in band intensity may result from DSB-dependent fragments being converted to other DNA species with different migration. This could result from the hyper resectioning of DSB ends (see [2,23]). Clarification of the nature of this putative intermediate must await its analysis at defined DSB hotspots, which we have yet to detect.
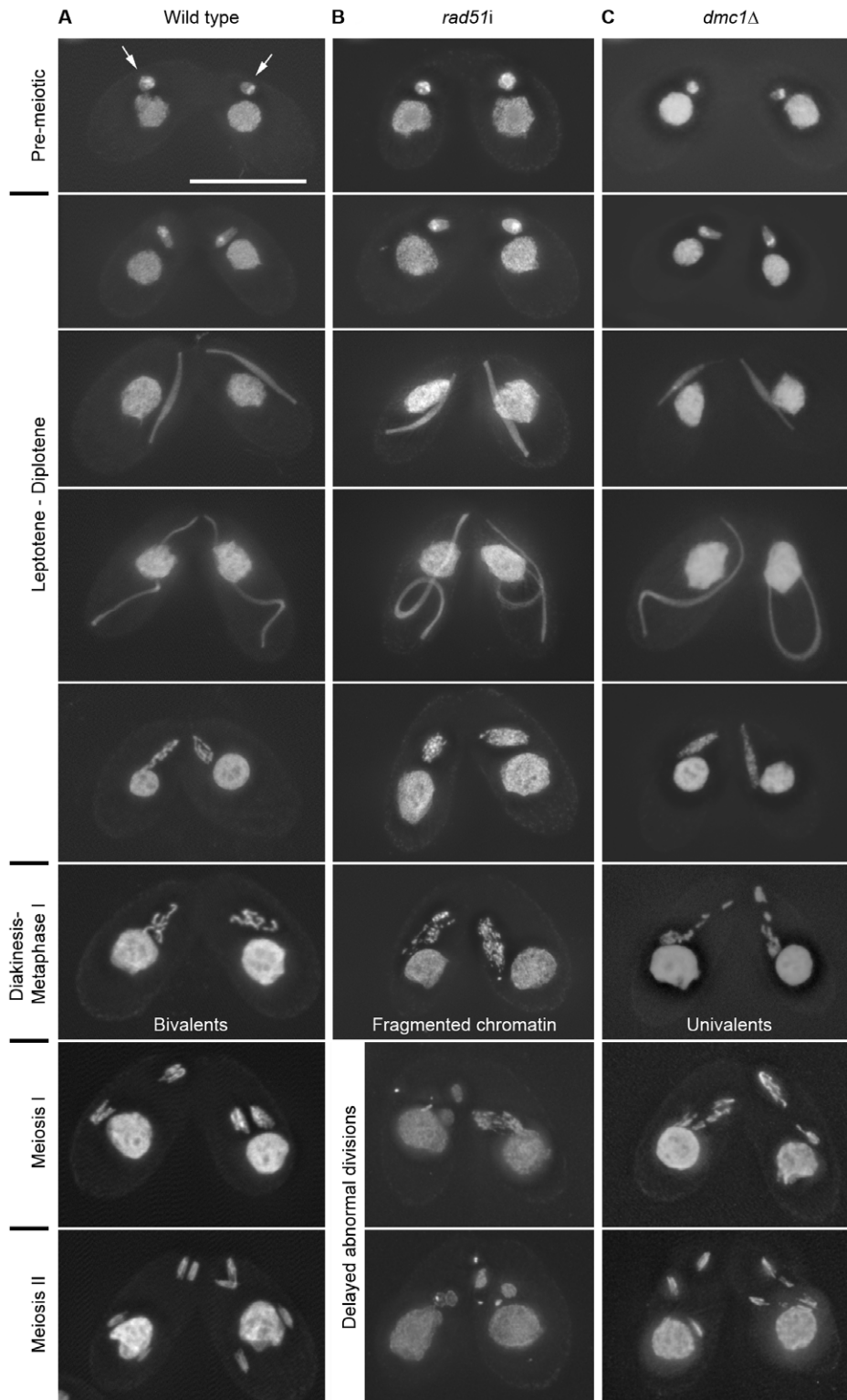
Figure 2. Stages of meiosis in *Tetrahymena* wild-type and mutant cells. Each panel shows two conjugating cells with their generative micronuclei (arrows) synchronously undergoing meiosis. Meiotic prophase culminates in an enormous elongation of the generative nuclei, within which chromosomes are arranged in a bouquet-like manner, and homologues become paired [25]. (A) In the wild type, prophase is followed by the emergence of 5 distinct bivalents (see Figure 3) and their separation during first and second meiotic division. In *rad51*i and *dmc1*Δ cells (B, C), prophase is morphologically normal, but at metaphase I, chromatin becomes fragmented in *rad51*i and univalents are formed in *dmc1*Δ (see Figure 3). *dmc1*Δ univalents are then (probably randomly) segregated during the first meiotic division whereas *rad51*i cells arrest with fragmented chromatin masses at a metaphase I-like stage. Only after an ~2 h delay, *rad51*i nuclei manage to undergo highly abnormal meiotic divisions. DAPI staining, bar indicates 10 μm.
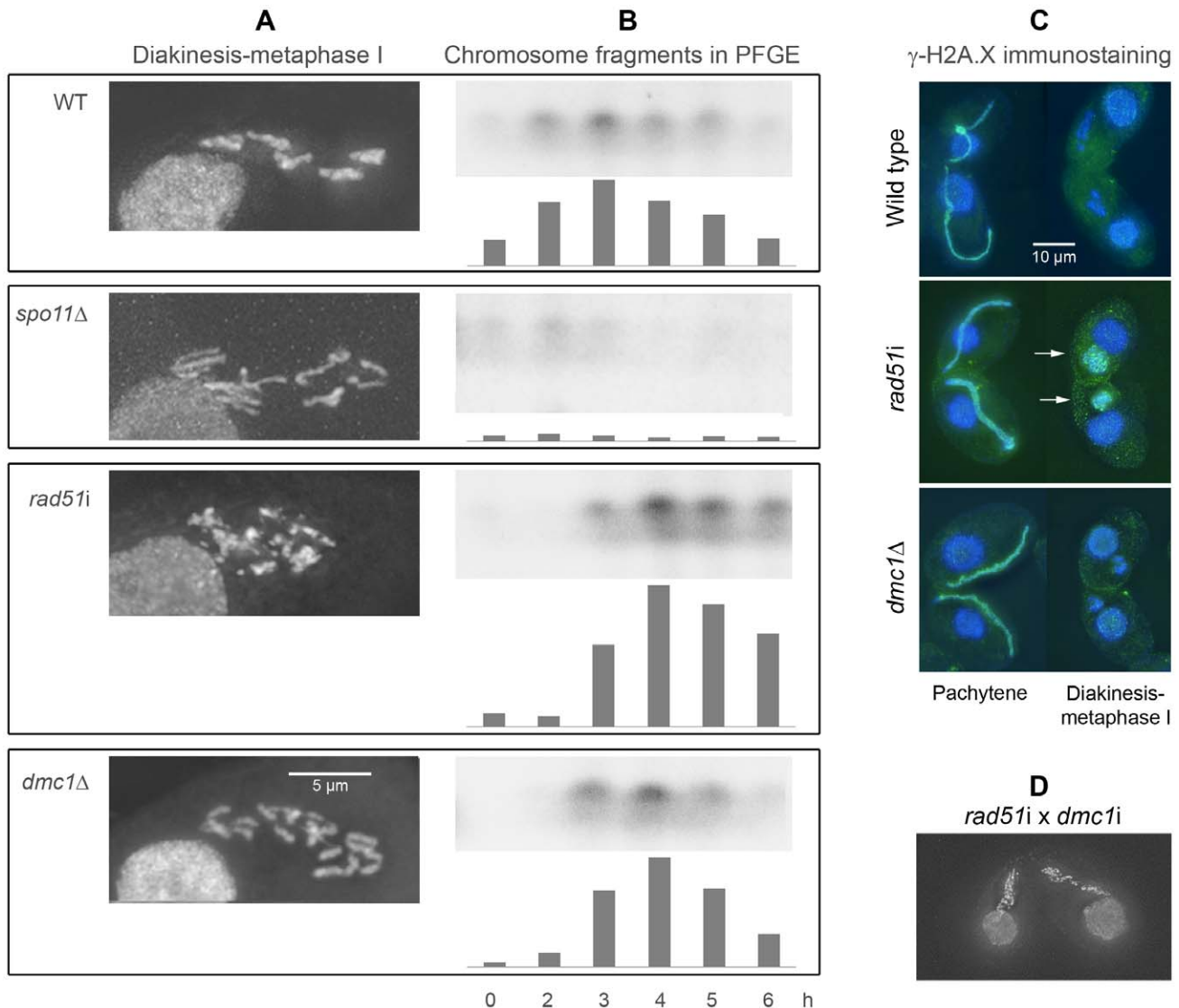
doi:10.1371/journal.pgen.1001359.g002

Figure 3. Diakinesis-metaphase I chromosome structure and DSB detection in the wild type and in mutants. (A, B) In the wild type, 5 bivalents are formed during diakinesis-metaphase I, and a band diagnostic of DSBs (see text) appears in a pulsed-field gel 2–3 h after induction of meiosis. It disappears by 6 h, i.e., at a time when the majority of cells are in metaphase I or later (see Figure S4). In the *spo11Δ* mutant, univalents appear because DSBs and crossovers are not formed. In *rad51*i meiosis, chromosomes appear fragmented, which is probably due to the failure to repair DSBs. Accordingly, DSB-dependent fragments do not disappear. (The fact that PFGE bands become slightly weaker late in meiosis may be due to some processing of DSB ends - see text). Like the *spo11Δ* mutant, the *dmc1Δ* mutant forms univalents. However, in this case, PFGE shows that DSBs are formed and repaired. Bar graphs indicate band intensities corrected for the amount of DNA loaded (see Figure S6). (C) Dynamics of the DSB marker γ-H2A.X. Elongated (~leptotene-pachytene) nuclei are strongly decorated by staining for phosphorylated H2A.X (green). In the wild type and in the *dmc1Δ* mutant, γ-H2A.X disappears during metaphase whereas in *rad51*i cells it persists (arrows). (D) Meiotic nuclei of *rad51*i × *dmc1*i double-RNAi matings display the chromosome fragmentation phenotype.
doi:10.1371/journal.pgen.1001359.g003

As an additional test for DSB behavior, we analyzed the localization of phosphorylated histone variant H2A.X. Phosphorylation of H2A.X (γ-H2A.X) is a DSB marker (see [24] and lit. cit. therein). In the wild type, γ-H2A.X was most prevalent in elongated meiotic nuclei, but was virtually absent in metaphases (Figure 3C; see also [25,26]). Consistent with the persistence of DSBs, γ-H2A.X was present into aberrant metaphase I in *rad51*i (Figure 3C).

In *dmc1Δ* meiosis, univalents are formed and efficient DSB repair takes place

In the absence of Dmc1p, elongation of the generative nucleus occurred as in the wild type (Figure 2C). However, at diakinesis-metaphase I, univalents appeared instead of bivalents (Figure 2C, Figure 3A). These univalents subsequently went through two meiotic divisions (Figure 2C) during which they are presumably randomly segregated, with a small chance of generating genetically balanced viable progeny. Of 164 favorable metaphase I nuclei evaluated, 15 (9%) displayed fewer than the 10 entities expected if they contained only univalents. Therefore, we can not exclude the possibility of rare bivalent formation.

The elongation of meiotic nuclei is indicative of the occurrence of DSBs [25], while intact diakinesis-metaphase I univalents suggest that these DSBs are repaired (Figure 3A). We used the PFGE-DSB assay to test for the transient appearance of DSBs. It

confirmed that in *dmc1*Δ, DSBs appeared about 3 h after induction of meiosis and virtually disappeared by 6 h after induction of meiosis (Figure 3B), which is similar to the wild type. Also, γ-H2AX foci disappeared from *dmc1*Δ mutant meiotic nuclei after the exit from the elongated state (Figure 3C). Together with the production of some viable progeny (see above), these results suggest that efficient DSB repair takes place in *dmc1*Δ. However, the (almost complete) lack of bivalents suggests that this repair does not take place by homologous crossover recombination.

Homologous pairing is reduced in *dmc1*Δ and *rad51*i mutants

The formation of univalents in the *dmc1*Δ mutant and the persistence of chromosome fragments in *rad51*i indicated that in neither case did DSB repair occur via crossing over with the homologous chromosome. Homologous strand invasion by ssDNA not only initiates crossover, but in many organisms also confers precise meiotic pairing [27,28]. Therefore, we tested if pairing was affected in the absence of Dmc1p and Rad51p. To this end, we determined the pairing of FISH-labeled homologous loci in fully elongated meiotic nuclei (Figure 4A). We found that pairing was reduced in *dmc1* and *rad51* deficiencies (Figure 4B), like in *mre11* and *com1* mutants where homologous strand exchange failed to take place [13]. This is consistent with our previous finding that the parallel, bouquet-like arrangement of chromosomes within the elongated meiotic nucleus is not sufficient to bring about precise homologous alignment, and that strand exchange may be required for homologous recognition and stable pairing [29].

Rad51p and Dmc1p localize to meiotic nuclei independently of DSBs

Having established that *RAD51* is essential for meiotic DSB repair, whereas *DMC1* is required for its homologous recombination outcome, we wanted to study the localization of the two proteins in meiotic nuclei. To this end, we used several antibodies and tags for their detection.

First, we used a commercial antibody (see Materials and Methods), which detects Rad51p in somatic nuclei (see above). When we applied this antibody to Western blots of meiotically expressed proteins, we found that it recognizes not only Rad51p but also Dmc1p (Figure 1C), which shares a 32% similarity with the former over a length of 328 amino acids. In cytology, this antibody labeled meiotic nuclei of wild-type cells (Figure 5A).

When we applied the anti-Rad51/Dmc1 antibody to *rad51*i cells, it stained the meiotic nucleus (Figure 5B). Since RNAi efficiently depleted Rad51p (Figure 1 and Figure S1), this labeling must be due to Dmc1p. Conversely, labeling was found in *dmc1*Δ meiotic nuclei as well (Figure 5C), in which case it must be due to the exclusive presence of Rad51p. It was noticed that staining of Dmc1p produced a granular pattern (Figure 5B), whereas Rad51p staining of the meiotic nuclei was more uniform (Figure 5C).

Notably, the anti-Rad51/Dmc1 antibody labeled meiotic nuclei of all stages from the beginning of their elongation (~ leptotene) to well beyond anaphase I, and it highlighted chromatin and chromatin-free regions (Figure 5D). To find out if this staining pattern reflects the actual distribution and temporal appearance of Rad51p and/or Dmc1p, we generated a specific anti-Rad51 antibody (data on the specificity of the antibody are summarized in Figure S3), and we tagged Rad51p with HA. As with the commercial antibody, we observed ubiquitous staining of meiotic nuclei during prophase and beyond, and sporadic spots in somatic nuclei (Figure 5E, 5F). Moreover, both antibodies labeled meiotic nuclei of *spo11*Δ cells (which are lacking DSBs) (Figure 5G). This confirms our previous observation [25] that Rad51p localizes to meiotic nuclei independently of the presence of DSBs.

To specifically study Dmc1p localization, we tagged this protein with mCherry. Dmc1-mCherry localized to chromatin and chromatin-free regions of meiotic nuclei but not to somatic nuclei (Figure 5H). Thus, Rad51p and Dmc1p are expressed and can be detected in meiotic nuclei even if they do not assemble near DSBs.

Dmc1p assembles in foci on chromatin independently of Rad51p

To detect if, in addition to their ubiquitous presence in meiotic nuclei, a subset of Rad51p and Dmc1p would localize to DSBs, we applied a detergent spreading method to remove soluble protein. Upon staining with the Rad51/Dmc1 antibody, spread wild-type meiotic nuclei displayed numerous foci (Figure 6A). On the other hand, signals were lost in spread *spo11*Δ meiotic nuclei (Figure 6B), demonstrating the removal of protein that was not bound to chromatin (compare with the unspread nuclei in Figure 5G). Unlike in conventionally prepared nuclei, no staining was detected at metaphase I or later in spread wild-type meiotic nuclei (data not shown). Together, this suggests that Rad51p and/or Dmc1p are associated with chromatin only in the presence of DSBs. Therefore, to eliminate background staining from recombination proteins that were present all over the nucleus, the following
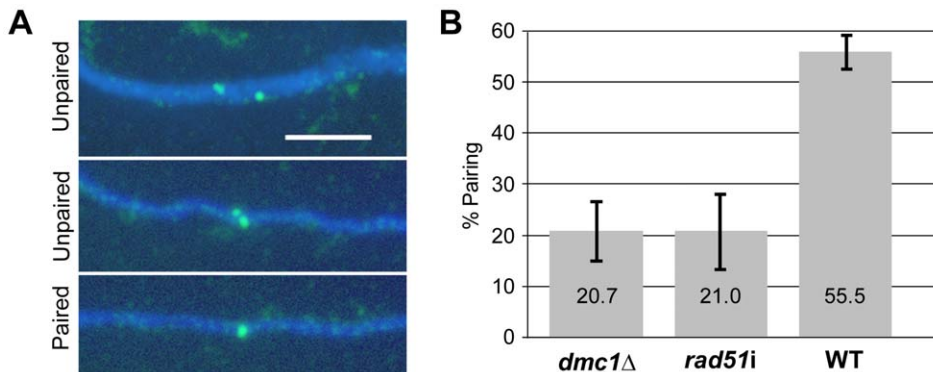
Figure 4. FISH to a chromosomal locus to evaluate homologous pairing in elongated meiotic nuclei. (A) Separate FISH signals (green) indicate unpaired loci whereas a single FISH signal indicates pairing (all examples from the wild type). Bar: 10 μm. (B) In the *dmc1*Δ mutant and in *rad51*i, pairing is reduced as compared to the wild type. Values are a mean of four experiments per genotype, with 50 nuclei evaluated in each counting and standard deviations indicated.
doi:10.1371/journal.pgen.1001359.g004

Figure 5. Detection of Dmc1p and Rad51p in conventionally prepared cells. (A–C) In cells of the wild type, *rad51*i and *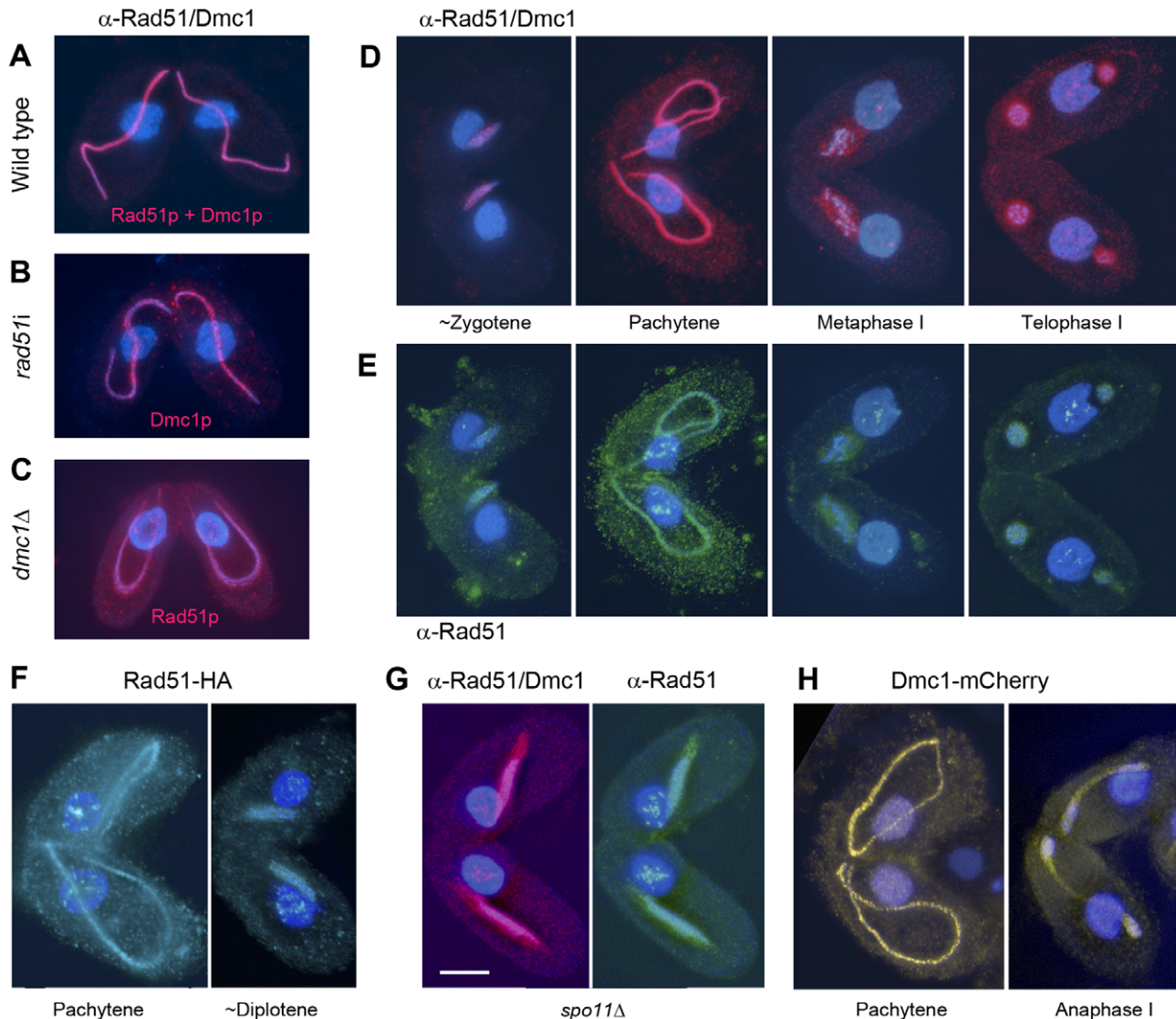dmc1*Δ strains, meiotic nuclei are immunolabeled by an antibody to Dmc1p and Rad51p red). Labeling of the wild-type meiotic nuclei (A) is due to the presence of both Dmc1p and Rad51p, whereas labeling of *rad51*i and *dmc1*Δ nuclei (B, C) is due to the exclusive presence of Dmc1p and Rad51p, respectively. (D, E) The anti-Rad51/Dmc1 (red) and a specific anti-Rad51 antibody (green) label meiotic nuclei from the beginning of elongation until well after anaphase I. (D and E show the same nuclei after double immunostaining.) (F) Examples of meiotic nuclei highlighted by Rad51-HA tagging (cyan). (G) In *spo11*Δ meiosis, anti-Rad51/Dmc1 (red) and anti-Rad51 (green) labels the meiotic nucleus (which does not fully elongate), which indicates that the expression of the recombination proteins is independent of the presence of DSBs. (H) Localization of mCherry-tagged Dmc1p (yellow) confirms the ubiquitous presence of this protein in meiotic nuclei. Note also the sporadic appearance of Rad51p (but not of Dmc1p) dots or patches in the somatic nucleus (C–G). Bar in G represents 10 μm in all images.
doi:10.1371/journal.pgen.1001359.g005

studies on the participation of Rad51p and Dmc1p in recombination foci were performed on spread nuclei.

To test the extent of Dmc1p contribution to the foci, we constructed cells expressing Dmc1-mCherry. Dmc1p localized to spread meiotic chromatin in numerous strong foci (Figure 6C). Foci were present from the beginning of elongation to shortly before diakinesis-metaphase. 100% of fully elongated nuclei (n = 100 nuclei longer than the cell) displayed strong foci.

Since it is possible, although unlikely, that Dmc1p focus formation was caused by the mCherry tag, we independently localized Dmc1p by applying the Rad51/Dmc1 antibody to *rad51*-RNAi cells, where it only highlights Dmc1p. Also in this experiment, Dmc1p was found assembled into numerous foci

(Figure 6D), with 100% of fully elongated meiotic nuclei (n = 100) displaying foci. Moreover, it also demonstrated that Dmc1p forms strong foci in the absence of Rad51p. To further confirm the independence of Dmc1p localization on Rad51p, we performed a *rad51*i × *DMC1-mCherry* crossing (where both conjugating cells are depleted of Rad51p and incorporate mCherry-tagged Dmc1p). Meiotic nuclei displayed strong Dmc1p foci in this case as well (Figure 6E). We quantified the brightness of Dmc1p foci by measuring gray values of foci on images (see Materials and Methods). They were 183 ± 18.5 (*DMC1-mCherry* × *rad51*i, n = 110 foci from 10 nuclei) vs. 177 ± 21.1 (*DMC1-mCherry* × wild type, n = 110 foci from 10 nuclei), hence Dmc1p signal intensity was found to be not reduced in the absence of Rad51p.
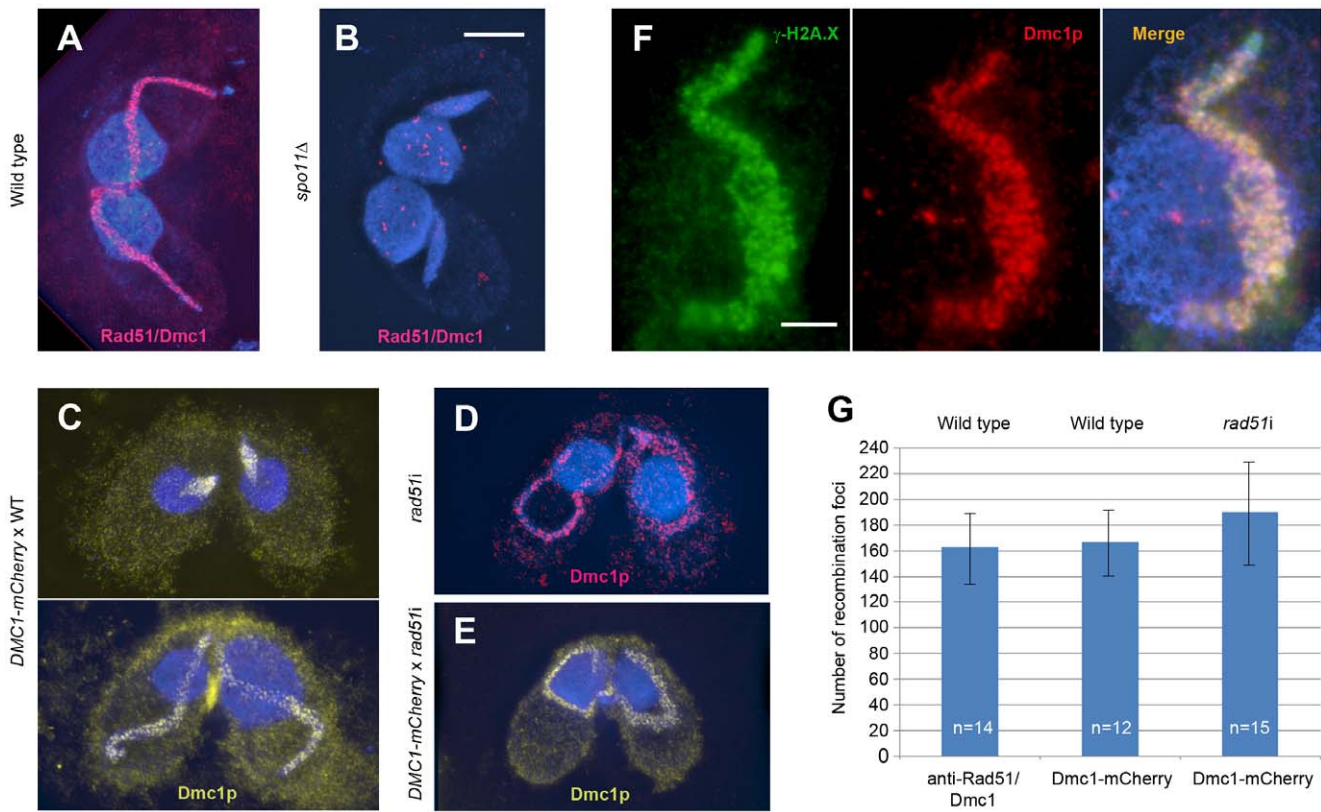
Figure 6. Localization of Dmc1p in spread cells. In detergent-treated samples, the anti-Rad51/Dmc1 antibody highlights foci in meiotic nuclei of the wild type (A) but not of *spo11Δ* (B), suggesting that Dmc1p and/or Rad51p are associated with chromatin only during wild-type meiosis. (C) Cells stained for mCherry-tagged Dmc1p. Top to bottom: Dmc1p focus formation starts right after initial elongation of the meiotic nuclei, and there is maximal abundance of foci in fully elongated nuclei. (D) In the *rad51*i strain, the anti-Rad51/Dmc1 antibody produces foci in the meiotic nucleus due to the exclusive presence of Dmc1p. (E) In Dmc1-mCherry × *rad51*i matings, where both partners are depleted of Rad51p, strong Dmc1p foci are formed. (F) Dmc1p foci colocalize with g-H2A.X dots. (G) Frequencies of Dmc1p recombination foci in wild-type (WT) and *rad51*i matings as determined by the detection methods indicated (n denotes the number of nuclei scored). Bar in b represents 10 μm in A, B and C–E; bar in F represents 5 μm.
doi:10.1371/journal.pgen.1001359.g006

It is likely, yet unproven, that nuclear foci of recombination proteins localize to DSB sites (for discussion see [1,30]). To corroborate this theory, we attempted to colocalize Dmc1p foci with γ-H2A.X, which occurs in chromatin flanking a DSB (see [24]). In spread nuclei, γ-H2A.X formed patches. Double staining with Dmc1p revealed a high degree of colocalization: of 431 Dmc1p foci scored in four different meiotic nuclei, 394 (91%) localized to a γ-H2A.X patch (Figure 6F).

To obtain an estimate of the number of DSBs that occur in *Tetrahymena* meiotic nuclei, we investigated the number of Dmc1p foci in spreads of wild-type and *rad51*i matings. There were, on average, 174 Dmc1p recombination foci per meiotic nucleus (Figure 6G). The number of Dmc1p immunostained foci in the wild type was not significantly different from the number of Dmc1-mCherry foci in *rad51*i (Figure 5D), which is additional evidence for the independence of Dmc1p localization on Rad51p.

Rad51p foci do not form on meiotic chromatin and are not triggered by experimentally induced DNA damage

To detect if Rad51p associates with meiotic chromatin, we stained spread cells with the specific anti-Rad51 antibody. In contrast to Dmc1p, Rad51p foci were virtually absent from meiotic nuclei. However, the presence of Rad51p signals in the somatic nuclei of the same cells indicated that immunostaining was working and that the spreading procedure did not remove Rad51p altogether (Figure 7A). In quantitative terms, none of 200 evaluated fully elongated (i.e., longer than the cell), meiotic nuclei displayed any foci. Similarly, we did not observe Rad51p foci in meiotic nuclei of *dmc1Δ* cells stained with the Rad51p/Dmc1p antibody (which, in this case, exclusively highlights Rad51p) (Figure 7B) or of strains expressing HA-tagged Rad51p (Figure 7C). In all these cases, foci were present only in somatic nuclei. Double staining of tagged Rad51p and Dmc1p revealed the distinct localization of these two proteins in one and the same cell (Figure 7D). The failure to detect meiotic Rad51p foci by three different cytological approaches suggests that Rad51p is much less abundant at DSBs than Dmc1p.

Only occasionally did we observe very weak Rad51p foci in barrel- or spindle-shaped meiotic nuclei of an uncertain stage (Figure 7A). At t = 2.5 h, 5% (n = 100) and at t = 4 h, 16% (n = 100) of barrel- or spindle-shaped meiotic nuclei displayed foci. The greater abundance of such nuclei at the later timepoint (when most nuclei have progressed beyond the maximal elongation stage - [13]; Figure S4 and compare Figure 2) suggests that a subset of meiotic nuclei develop Rad51p foci after maximal elongation and hence much later than the first appearance of Dmc1p foci. The sporadic occurrence of these cells could indicate that a small amount of Rad51p is associated with meiotic DSBs during a short period late in meiotic prophase and/or in a subset of cells that fail to undergo
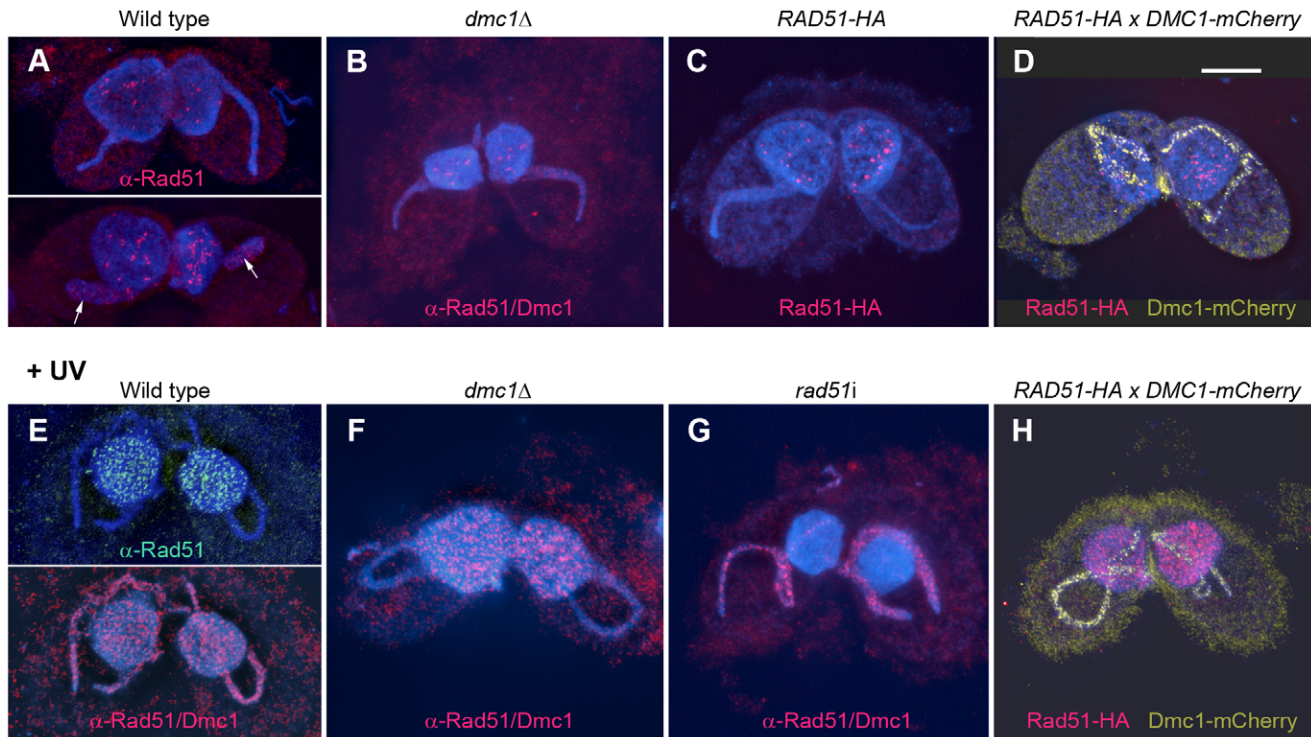
Figure 7. Localization of Rad51p in spread cells. Rad51p is not detected in spread pachytene nuclei whereas it is present in vegetative nuclei. This suggests that, while Rad51p is present in the meiotic nucleus (Figure 5), visible amounts of it do not associate with DSBs. (A) Top: Rad51p foci are not detected in fully elongated meiotic (~pachytene) nuclei by immunostaining with a specific anti-Rad51 antibody. Bottom: Rare nuclei at a later stage (see text) display weak foci (arrows). (B) Rad51p foci are not detected in meiotic nuclei of *dmc1*Δ strains. (C) HA tagging of Rad51p fails to show meiotic foci. (D) Double staining of Rad51-HA and Dmc1-mCherry confirms the inability of Rad51p to assemble on meiotic chromatin, whereas Dmc1p forms foci exclusively in the meiotic nucleus. (E–H) UV-radiation applied to increase *RAD51* expression. (E) Top: With the Rad51p antibody there is strong labeling only of somatic nuclei. With the Rad51p/Dmc1p antibody, there is strong Rad51p labeling in the somatic nuclei of the wild type (E, bottom) and of the *dmc1*Δ mutant (F). (G) No Rad51p signal is found in the somatic nuclei of the *rad51*i strain. (H) Double staining of Rad51-HA and Dmc1-mCherry confirms that, while UV induces Rad51p foci in the somatic nucleus, it fails to do so in the meiotic nucleus. This demonstrates that even under conditions of increased DNA damage in meiotic nuclei and of Rad51p induction (see Figure S1C), there is no association of visible Rad51p foci with DSBs. Chromatin is stained blue with DAPI. Bar represents 10 μm.
doi:10.1371/journal.pgen.1001359.g007

normal meiosis. The weakness of these foci, at the limit of detectability, precluded their quantification.

As mentioned before, efficient DSB repair takes place in *dmc1*Δ meiosis, while at the same time prominent Rad51p foci are absent (Figure 7C). Thus, there does not seem to occur a compensatory Rad51p localization to DSBs. Therefore, it might be argued that the absence of Dmc1p triggers an alternative Rad51p-independent repair process such as single-strand annealing [31] or non-homologous end-joining. To exclude this possibility, we created a *dmc1*i strain and mated it to *rad51*i, creating a situation where meiotic cells are depleted of both proteins. In these double-deficient meioses, diakinesis-metaphase I chromosomes were fragmented just as in *rad51*i (Figure 3D), indicating that DSB repair did not take place and that Dmc1p-independent repair requires Rad51p.

If there was an undetectably low amount of Rad51p associated with meiotic DSBs, it might be possible to increase it above the threshold of visibility by inducing additional DNA damage. Therefore, we exposed cells to 25 J/m^2 UV-C prior to meiosis and tested for Rad51p focus formation. We found that UV irradiation induced strong foci (detected by the specific anti-Rad51 antibody) in somatic nuclei, whereas it failed to do so in meiotic nuclei (Figure 7E, top). Likewise, the Rad51/Dmc1 antibody highlighted foci in the somatic and the meiotic nuclei of the wild type (Figure 7E, bottom), but only in the somatic nuclei of *dmc1*Δ

cells (Figure 7F). This, again, confirms that the foci detected in meiotic nuclei of the wild type consisted of Dmc1p only. Conversely, no foci were produced by Rad51/Dmc1 immuno-staining in the somatic nuclei of irradiated *rad51*i cells, indicating that RNAi was efficient, and that UV does not induce Dmc1p in the somatic nucleus (Figure 7G). The exclusive expression of UV-induced Rad51p in the somatic nucleus and of Dmc1p in the meiotic nucleus was also seen by the simultaneous detection of HA-tagged Rad51p and mCherry-tagged Dmc1p (Figure 7H). Altogether, UV irradiation induced strong Rad51p foci in 100% of the somatic nuclei (n = 100), whereas only 5% of meiotic nuclei (n = 100) displayed very faint Rad51p staining. Similarly, bleomy-cin (50 μg/ml), which we previously had shown to produce DSBs in the generative nucleus [13], induced Rad51p foci in somatic nuclei but not in meiotic nuclei (data not shown). Thus, DNA damage seems to trigger different processing of lesions in nonmeiotic and meiotic nuclei, with less Rad51p involvement in the latter.

A proximity ligation assay fails to detect colocalization of Dmc1p and Rad51p

The absence of Rad51p foci from spread meiotic nuclei strongly suggests that very little Rad51p is associated with DNA at DSBs. However, there remains the unlikely alternative that spreading

removes chromatin-associated Rad51p but not Dmc1p, and that this loss affects meiotic nuclei, but not somatic nuclei. Therefore, we wanted to confirm the low abundance of Rad51p associated with meiotic chromatin by an independent approach, the proximity ligation method. In this method, oligonucleotides attached to antibodies against two target proteins ligate and can be amplified to multiple DNA circles when bound in close proximity, i.e., separated by ∼40 nm or less. These polymers are visualized by the incorporation of fluorescence-labeled nucleotides (for the principle of the method see [32] and Figure S5).

We performed the assay on conjugating wild-type cells carrying both Rad51-HA and Dmc1-mCherry and conventionally prepared for microscopy. To detect Rad51p-Dmc1p colocalization, cells were labeled with anti-Dmc1-mCherry and anti-Rad51-HA (Figure 8, Table 2). For control experiments, antibody pairs were used which detected the same protein: anti-Dmc1-mCherry and anti-Rad51p/Dmc1p to mark Dmc1p, anti-Rad51-HA and anti-Rad51p to mark Rad51p (Figure 8, Table 2).

Signals produced by the proximity ligation assay were less abundant than those from immunostaining (Figure 8), presumably because of a threshold of local antigen concentration required to support the reaction. Although Rad51p was found to be abundant in unspread meiotic nuclei by immunostaining (see above), the proximity ligation assay detected significantly fewer Rad51p-dependent signals (Figure 8A) than Dmc1p-dependent signals (Figure 8B, Table 2). This is consistent with the possibility that non-chromatin-associated Rad51 molecules are dispersed in the nucleus, but their local concentration is not sufficient to develop a signal. Of the few Rad51p-dependent signals detected, a large proportion localized to the somatic nucleus (Figure 8A). This is consistent with the detection of Rad51p in a subpopulation of somatic nuclei by immunostaining (see above). In contrast to Rad51p, numerous Dmc1p-dependent signals were produced in meiotic nuclei (Figure 8B), suggesting that a substantial amount of the protein forms clusters, such as would be expected from nucleoprotein filaments. Only a few signals were produced after combining antibodies detecting Dmc1p and Rad51p (Figure 8C). The scarcity of reaction products confirms the conclusion from

immunostaining that Dmc1p and Rad51p form few, if any, mixed nucleoprotein filaments.

Discussion

Large amounts of Dmc1p, but barely detectable amounts of Rad51p, localize to meiotic DSBs

In all organisms where the localization of Rad51 or Dmc1 recombinases has been studied so far, they appear as nuclear foci, and impressive circumstantial evidence suggests that these foci reflect the association of protein complexes with DSBs (see [1,30]). Here, we found that in *Tetrahymena*, there is abundant expression of Dmc1p and Rad51p in meiotic nuclei. The bulk of the two proteins localized throughout the nuclei including chromatin-free regions, and their presence was independent of DSBs. However, when we applied preparation conditions under which free nuclear proteins are removed, numerous DSB-dependent Dmc1p foci, but virtually no Rad51p, remained associated with meiotic chromatin. On the other hand, Rad51p foci were readily detectable in the somatic nuclei within the same cells (for a graphical summary see Figure 9).

Independent experiments using HA-tagged Rad51p, a specific antibody against Rad51p, or a Rad51p/Dmc1p antibody (applied to *dmc1Δ*) all failed to detect meiotic Rad51p foci. This was not due to deficits in the reporter systems since all three approaches detected Rad51p clusters in the somatic nucleus. In contrast to Rad51p, strong meiotic Dmc1p foci were observed by Dmc1p tagging and with the antibody against Rad51p/Dmc1p. Similarly, a proximity ligation assay produced abundant signals associated with meiotic nuclei only for Dmc1p, whereas it detected Rad51p in somatic nuclei. Together, this suggests that Dmc1p is much more abundant than Rad51p at meiotic DSB sites.

Despite the well-established correlation between cytological foci and DSBs, it is not clear if cytological foci represent recombination proteins that form nucleoprotein complexes with ssDNA at DSBs (see [1,33]). Some support for the equivalence of nucleoprotein filaments and foci comes from the observation that focus formation was strongly reduced in *mre11Δ* and *com1Δ* mutants [13] where
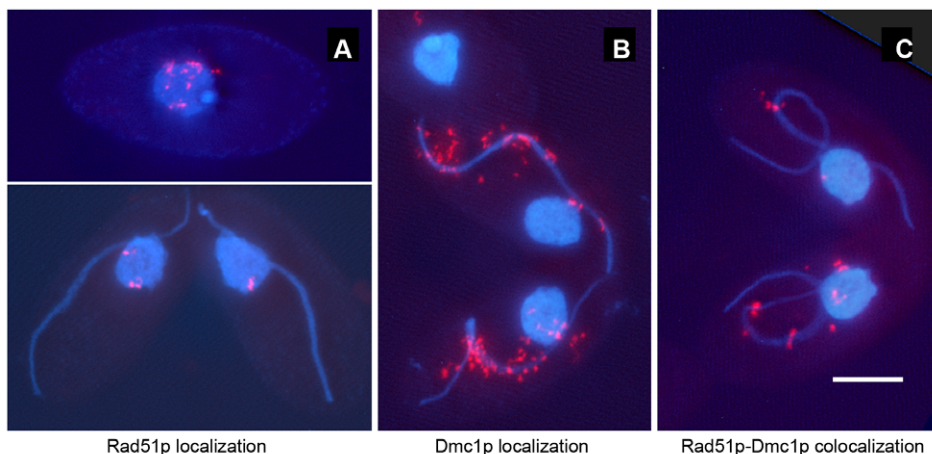

Rad51p localization   Dmc1p localization   Rad51p-Dmc1p colocalization

Figure 8. Detection of Rad51p-dependent and Dmc1p-dependent signals by the proximity ligation assay. Signals consisted of groups of connected spots extending from the target, probably as a consequence of the amplification process building large DNA complexes. (A) Rad51p signals (generated by the combination of α-Rad51-HA and α-Rad51p) are common in somatic nuclei of vegetative cells (top), and are also present in some somatic nuclei in meiotic cells (bottom). They are relatively rare in elongated meiotic nuclei (bottom; see Table 2). (B) Dmc1p signals (generated by the combination of α-Dmc1-mCherry and α-Rad51p/Dmc1p) are mostly found associated with fully elongated meiotic nuclei. (C) Signals depending on the proximity of Dmc1p and Rad51p (generated by the combination of α-Dmc1-mCherry and α-Rad51-HA) are rare (see Table 2). Bar: 10 µm.
doi:10.1371/journal.pgen.1001359.g008

Table 2. Localization of Rad51p and Dmc1p by the proximity ligation assay.

Experiment	No. of signals/25 cells	No. of signals/cell	No. of signals/cell (% of signals) associated with		
			Meiotic nuclei	Somatic nuclei	Cytoplasm
Rad51p localization (α-Rad51-HA + α-Rad51p)	81	3.24	1.24 (38)	1.0 (31)	1.0 (31)
Dmc1p localization (α-Dmc1-mCherry + α-Rad51p/Dmc1p)	238	9.52	8.36 (88)	0.32 (3)	0.84 (9)
Rad51p-Dmc1p colocalization (α-Rad51-HA + α-Dmc1-mCherry)	52	2.08	1.08 (52)	0.12 (6)	0.88 (42)

Only cells with maximally elongated meiotic nuclei were used for evaluation. In each experiment, the 25 cells with the most signals, selected out of >500 cells per slide, were evaluated. Signals in the cytoplasm may represent recombination proteins that have not yet been imported into the nuclei.
doi:10.1371/journal.pgen.1001359.t002

ssDNA resection and single-strand exposure are believed to be reduced (see [13]). Moreover, here we showed that Dmc1p foci localize to patches of γ-H2A.X, which in turn appears around DSBs [24]. Thus, if the presence and strength of foci reflected the amount of protein involved in filament formation, the proportion of Rad51p in nucleoprotein filaments must be small as compared to Dmc1p. The alternative explanation, that Dmc1p foci might be more resistant to preparation- related loss than Rad51p foci, is
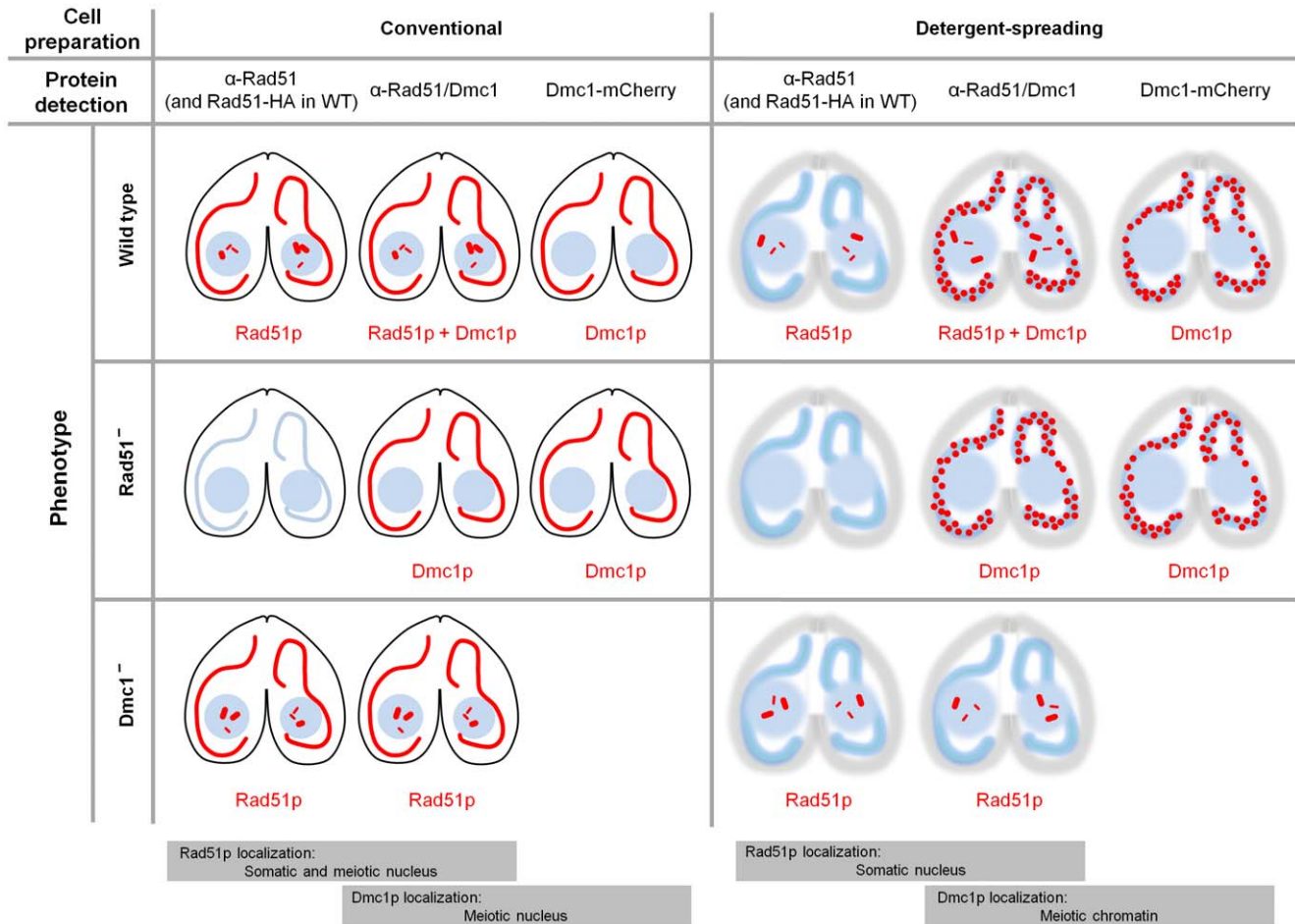

Figure 9. Summary of Rad51p and Dmc1p localization. Immunostaining or protein tagging of Rad51p and/or Dmc1p were performed on conjugating (meiotic) cells expressing both or only one of the two proteins to reveal the specific localizations of Rad51p and Dmc1p. In addition, conventional preparation and detergent spreading were applied to discriminate between soluble and chromatin-bound protein fractions. Depicted in red are the localizations of Rad51p and/or Dmc1p as tested by various combinations of protein detection and preparation methods for each phenotype. Conventional preparation revealed a homogeneous distribution of both Rad51p and Dmc1p in meiotic nuclei and the presence of Rad51p spots or patches in somatic nuclei. Spreading washed out Rad51p from meiotic but not from somatic nuclei. Dmc1p was retained as foci in spread meiotic nuclei. From these observations we conclude that Rad51p occurs in somatic and in meiotic nuclei whereas Dmc1p occurs only in meiotic nuclei. In meiotic nuclei, Dmc1p foci are associated with chromatin (most likely at DSBs) whereas most or all of Rad51p is dispersed in the nuclear lumen.
doi:10.1371/journal.pgen.1001359.g009

rendered less likely due to the similar physical properties of Dmc1- and Rad51-ssDNA filaments in vitro [34].

Strikingly, Rad51p foci were not detected on meiotic chromatin even after artificial induction of DNA lesions, whereas Rad51p formed numerous strong foci on somatic chromatin under these conditions. This suggests that in the meiotic nucleus, a specific regime prevails that prohibits the association of large amounts of Rad51p with damaged DNA, perhaps in the interest of promoting homologous over sister repair.

In meiotic nuclei of budding yeast, Shinohara et al. [35] found foci that contained Rad51 and Dmc1 side-by-side, leading them to propose that Rad51 and Dmc1 each form homo-oligomers rather than mixed complexes at recombination sites. Our failure to observe meiotic Rad51p foci suggests that long, pure Rad51p nucleoprotein filaments do not form in *Tetrahymena*, and is consistent with short (and perhaps transient) Rad51p filaments or mixed filaments with Dmc1p predominating. Moreover, the proximity linkage assay for Dmc1-mCherry and Rad51p produced very little signal, which suggests that little if any Rad51p colocalizes with Dmc1p, and argues against the abundant presence of Rad51p in mixed nucleoprotein filaments.

Unlike in the budding yeast and in *Arabidopsis* [36,37], strong Dmc1p foci did form even in the absence of Rad51p. This suggests that Dmc1p does not require Rad51p for its polymerization along ssDNA. However, abundant loading of Dmc1p is not sufficient for the repair of meiotic DSBs in the absence of Rad51p.

Rad51p is required for the repair of meiotic DSBs

Despite the fact that Rad51p does not assemble in cytologically visible recombination foci, suggesting that it is not present at notable amounts at DSBs, it is indispensable for meiotic DSB repair and recombination. In the absence of Dmc1p, Rad51p is sufficient to allow efficient repair, however, a compensatory accumulation of Rad51p does not occur. This is in contrast to budding yeast *dmc1Δ* strains, where bright Rad51p foci are formed [38]. It may be assumed that if Dmc1p is missing, repair takes place via the sister chromatid and requires only minimal Rad51p nucleoprotein filament formation, below cytological detectability.

In the wild-type situation, when Dmc1p is present, Rad51p is necessary to support interhomolog crossover recombination. It is conceivable that this is achieved by Rad51p somehow activating Dmc1p at DSBs, without being incorporated in nucleoprotein filaments. Alternatively, a small number of Rad51p molecules, below cytological detection, might be part of these nucleoprotein filaments.

Dmc1p may form long nucleoprotein filaments to promote interhomolog crossover recombination

In the absence of Dmc1p, we observed intact univalents during diakinesis to metaphase I. Accordingly, 3.4% viable sexual progeny were produced by *dmc1Δ* meiosis, which is consistent with the random segregation of univalent chromosomes, which may provide a low percentage of progeny cells with balanced chromosome sets. Therefore, our observations provide strong support of efficient DSB repair in the absence of Dmc1p. While we cannot exclude the rare occurrence of bivalents in *dmc1Δ* meiosis, sporadic interhomologue recombination can not account for the complete disappearance of DSBs observed in the PFGE assay. Therefore, it is likely that this Dmc1-independent repair, like in budding yeast [2,39], preferentially takes place via the sister with the help of Rad51p, yet with only little Rad51p actually localizing to DSBs (see above).

Only in the presence of Dmc1p are bivalents regularly formed. Thus, Dmc1p is needed for recombination with the homologue.

The formation of strong Dmc1p foci during meiotic prophase invites the simple interpretation that long Dmc1p-containing nucleoprotein filaments are formed at DSBs. It is tempting to speculate that short Rad51p nucleoprotein filaments are sufficient for intersister recombination whereas long nucleoprotein filaments consisting primarily of Dmc1p are advantageous or even indispensable (but not sufficient) for interhomolog recombination.

Both in the presence or absence of Rad51p, ca. 170 Dmc1p foci were counted per meiotic nucleus (see Results). Data from budding yeast, where the maximum number of Dmc1-Rad51 foci was about 2.5-fold less than the average recombination frequency (CO + NCO), suggest that, because of their transient nature, recombination foci may underestimate recombination events [38,40]. Thus, it can be estimated that in *Tetrahymena* there occur 200 or more DSBs per meiosis, whereas the rod- or ring-shape of bivalents suggests that only a fraction are converted to chiasmata. In this respect, *Tetrahymena* resembles higher plants and animals such as maize, the lily, and the mouse, where a considerable excess of DSBs over crossovers/chiasmata was found [41–43].

Tetrahymena employs a conserved Dmc1-dependent homologue-directed recombination mechanism

For the success of meiosis it is essential that strand exchange takes place between homologous chromosomes rather than sisters, which would be the more readily available option. In the budding yeast, two mechanisms for the promotion of interhomolog recombination have been identified (see [3]). In one, the homolog-over-sister recombination preference is conferred by a not yet understood activity of Dmc1 [2]. In the other, an activation/phosphorylation cascade involving the Red1, Hop1, and Mek1 proteins at the axial elements of the SC impedes intersister exchange by Rad51 through phosphorylation of its binding partner, Rad54 (see [3,7,44–47]). Similarly, axial element proteins may be involved in recombination partner choice in the fission yeast [48] and in *C. elegans* [49]. Such an axial element-dependent barrier or impediment to unwanted intersister recombination is not universal, however. In *Arabidopsis dmc1* mutants, DSBs are readily repaired by a noncrossover pathway (possibly via the sister chromatid), even when the SC is in place [10,11].

In *Tetrahymena*, homologous chromatids are closely conjoined in the tubular meiotic prophase nucleus, with homologous loci in opposing positions [29]. Nevertheless, the cohesion of sister chromatids may cause their more intimate contact and an intrinsic preference for intersister recombination. Homologues of axial element proteins and SC-related structures have not been detected (see [25]), thus a mechanism involving axial elements to overcome the intersister bias may be lacking. Our data suggest that *Tetrahymena* shares with the budding yeast a Dmc1-dependent mechanism to promote a sufficient rate of interhomolog recombination. A simple physical model would pose that Dmc1p-containing nucleoprotein filaments are longer than those consisting of Rad51p and therefore are able to bridge the larger interhomolog distances.

Materials and Methods

Strain culture

Tetrahymena thermophila strains B2086 and CU428 served as wild types and as the source material for the construction of gene knockout and knockdown strains. *spo11* knockout (*spo11Δ*) lines were described previously [25]. Cells were grown in standard medium at 30°C [50]. For induction of conjugation and meiosis, cells of complementing mating types were starved in 10 mM Tris-

Cl (pH 7.4) for at least 16 h and mixed in equal amounts ($\sim 2 \times 10^5$ cells/ml).

Construction of *dmc1* knockout (*dmc1Δ*) strains

To create the *dmc1* knockout constructs, ~500 bp-fragments of genomic *Tetrahymena* DNA upstream and downstream of the *DMC1* open reading frame (ORF) were amplified using the following primers: DMC1KO5FW (5′-cag aag ttg cta gaa gc-3′), DMC1KO5RV (5′-gtc tat cga att cct gca gcc cgc ttt tca gtg cag cta g-3′), DMC1KO3FW (5′-ctg gaa aaa tgc agc ccg cct tct act ggt tga ttt-3′), and DMC1KO3RV (5′-gct gat aga tct aaa tga aat taa g-3′). These fragments were then joined to each end of the *neo4* selection cassette using overlapping PCR [51]. The knockout construct was introduced into B2086 and CU428 cells by biolistic transformation as described previously [52]. The *NEO4* resistance gene is expressed under the Cd^{2+}-inducible *MTT1* metallothionein promoter [53]. Transformants were selected in media containing 0.1 – 1 µg/ml $CdCl_2$ and increasingly higher concentrations of paromomycin (from 120 µg/ml to 10 mg/ml) until the wild-type chromosomes were completely replaced by the knockout chromosomes in the somatic nucleus.

RAD51 and DMC1 knockdown by RNA interference

To create the *rad51* RNAi construct, a ~500 bp-fragment of the *RAD51* ORF was amplified from genomic DNA using PCR primers to add appropriate restriction sites for cloning into the RNAi hairpin vector (PmeRad51FW 5′-cgt tta aac gaa aca ggc tct ctc act g-3′, ApaRad51FW 5′-cgg gcc cga aac agg ctc tct cac tg-3′, SmaRad51RV 5′-gcc cgg gcc gaa ttc gtc agc aag tc-3′, XhoRad51RV 5′-gct cga gcc gaa ttc gtc agc aag tc-3′). These fragments were then used to replace the *SERH3* fragments in the RNAi vector construct described previously [20]. The finished hairpin construct was introduced into mating cells by biolistic transformation at 10 hrs post-mixing to allow cells to process the rDNA vector [52,54]. Transformants were selected initially in media containing 120 µg/ml paromomycin, and then were transferred to increasingly higher concentrations, up to 600 µg/ml.

Expression of dsRNA under the *MTT1* promoter was induced by the addition of $CdCl_2$ (final concentration: 0.1 µg/ml) to cells carrying the hairpin construct (*rad51*hp). For *RAD51* knockdown in meiosis, $CdCl_2$ was added ca. 3 h after the beginning of starvation, i.e. when mitotic divisions had ceased. Since $CdCl_2$ was found to impair conjugation, the *rad51*hp cells were washed twice and resuspended in 10 mM Tris-Cl (pH 7.4) before mixing. For some experiments, two *rad51*hp lines of different mating types were mixed. For others, a *rad51*hp line was mated to lines not carrying the *rad51* hairpin construct. Because RNAi causes a systemic response in *Tetrahymena* [20], the construct-free partner also displayed the RNAi phenotype. Cells were harvested at appropriate times in meiosis. For controls, meiosis was induced in the wild type under the same regime of $CdCl_2$ treatment, and in *rad51*hp cells without $CdCl_2$ treatment. Meiosis was normal in $CdCl_2$-treated wild type. In *rad51*hp cells without $CdCl_2$, bivalents appeared somewhat less condensed, but meiotic divisions were not notably affected.

To induce Rad51p overexpression, cells were exposed to UV radiation (254 nm UV-C; 20 Joule/m²) using a Stratalinker UV crosslinker [29].

To study the *rad51-dmc1* double deficiency phenotype, a *dmc1*hp strain was created and mated to a *rad51*hp strain. The *dmc1* interfering RNA was constructed in the same way as the *rad51*hp. The primers used were: PmeDmc1FW 5′-cgt tta aac gag ttt gtt ctc ggt act ac-3′, ApaDmc1FW, 5′-cgg gcc cga gtt tgt tct cgg tac tac-3′, SmaDmc1RV 5′-gcc cgg gca gcc att ctt tat aat ctg ctc-3′, XhoDmc1RV 5′-gct cga gca gcc att ctt tat aat ctg ctc-3′. Expression of dsRNA was induced as described above.

Pulsed-field gel electrophoresis (PFGE)

To detect meiotic DSBs, DNA was separated by PFGE under conditions where intact chromosomes do not enter the gel, whereas DSB-dependent chromosome fragments of different sizes appear as a distinct band [13]. Chromosome-sized DNA was prepared in agarose plugs as described elsewhere [13]. Gels were run on a CHEF apparatus. Chromosomes of the generative nucleus were distinguished from the background of somatic minichromosomes (which are distributed throughout the gel) by Southern hybridization with a micronucleus-specific probe [13].

Tagging of Dmc1p and Rad51p, and Rad51p antibody production

DMC1-mCherry was created by fusing the mCherry red fluorescent protein gene to the C-terminus of the *DMC1* ORF. To create the tagging construct, the last ~500 bp of the *DMC1* gene (excluding the stop codon), and ~500 bp of DNA downstream of the *DMC1* gene were amplified from genomic *Tetrahymena* DNA using the following primers: 5AmDmc1FW (5′-gct gat ggc gat gaa tga aca ctg gct cta cta gtt gtt gat tca ata atg gc-3′), DMC1mCheRV (5′-gtt atc ttc ttc tcc ttt tga aac cat gga tcc acc agt aga agg ctt ttt atc aca ttc aac-3′), Neo4-Dmc1FW (5′-ccc ggg gga tct gaa ttc gat atc aag ctt gaa tat tct ttg aga aag tta gtt aaa tga-3′) and 3AmDmc1RV (5′-gcg agc aca gaa tta ata cga ctg ctg ata gat cta att gaa att aag aat ga-3′). These fragments were then joined to each end of the *mCherry-neo4* cassette (amplified from the *pmCherry-neo4* plasmid, gift of Kazufumi Mochizuki) using overlapping PCR. Tagged mCherry was at least partially functional, since matings of Dmc1-mCherry cells to *dmc1Δ* cells produced viable sexual progeny, although with a reduced frequency (Table 1).

Strains expressing Rad51-HA were created in a similar manner using the following primers and the *pHA-Neo4* plasmid (a gift from Kazufumi Mochizuki): 5′FW (5′-gct gca tgc gat gaa tga aca ctg ttc agc cac tgc tct tta c-3′), 5′RV (5′-aag ttc ttc acc ctt aga aac cat gga tcc ctc gtt gaa gtc ttc aat acc-3′), 3′FW (5′-ccc ggg gga tct gaa ttc gat atc aag ctt gct aaa aga taa taa gat aaa att c-3′) and 3′RV (5′-gcg gtc gac gaa tta ata cga cta tat tat att ggt ata aca tta ttt tat ag-3′). Transformations and selections were performed as for the knockout strains described above.

Antiserum was produced in rabbits against the peptide sequence AIYAIGKGGIEDFNE from the C-terminus of the Rad51 protein. This region has only low similarity to the related Dmc1p. The serum was immunopurified against the polypeptide (Eurogentec, Seraing, Belgium), and its specificity was confirmed by its failure to label nuclei of *rad51*i cells (Figure S3).

Western blotting

Protein extracts were prepared from 5 ml of conjugating cells by trichloroacetic acid precipitation. 20 µl of extracts were run on 10% SDS-PAGE gels and blotted to Hybond-P PVDF membrane (Amersham Biosciences). Proteins of interest were detected by incubating the blot for 2 h with anti-Rad51/Dmc1 antibody (1:200 mouse monoclonal, Clone 51RAD01, NeoMarkers, Fremont, CA) in TBST (20 mM Tris pH 7.5, 140 mM NaCl, 0.05% Tween 20) +1% dry milk, washing, incubating for 1 h with HRP-conjugated anti-mouse antibody (1:100.000), washing, then incubating with chemiluminescent reagent (Thermo Scientific), and exposing to X-ray film.

Standard cell preparation for microscopy

Following [22] and [18], 5 ml of a suspension of conjugating cells were fixed by the addition of formaldehyde and Triton X-100

(final concentrations of 4% and of 0.5%, respectively). After careful mixing, the cells were left for 30 min at room temperature, then centrifuged, and the pellet was resuspended in 500 µl of a solution of 4% paraformaldehyde and 3.4% sucrose in water. A drop of this mixture was spread on a clean slide and air-dried. These slides were used for nuclear staining with DAPI (4′,6-diamidino-2-phenylindole) or for immunostaining.

Cell spreading

For the cytological detection of chromatin-associated Dmc1p and Rad51p foci, a protocol for enhanced detergent spreading of cells was applied [13]. In short, a mixture of 450 µl of 10% Triton X-100 and 50 µl of 37% formaldehyde solution was quickly added to a tube with 5 ml of conjugating cells. The liquids were mixed by inverting the tube, and after 25 min on ice another 450 µl of formaldehyde solution were added. After 5 min the cells were pelleted and resuspended in 500 µl of a solution of 4% paraformaldehyde and 3.4% sucrose in water. Eighty microliters of this suspension were spread on a slide and allowed to dry.

Immunostaining

For immunostaining, slides prepared by either of the above methods were washed with 1× PBS and 1× PBS +0.05% Triton X-100, incubated with primary antibody for 3 h at room temperature or over night at 4°C, washed as above, incubated with Cy3- or FITC-labeled secondary antibody for 1.5 h–3 h at room temperature, washed again and mounted under a coverslip in Vectashield anti-fading agent (Vector Laboratories Inc., Burlingame, CA,) supplemented with 0.5 µg/ml DAPI as a DNA-specific counterstain. The primary antibodies were: anti-Rad51/Dmc1 (1:50 mouse monoclonal, Clone 51RAD01, NeoMarkers, Fremont, CA), anti-Rad51 (1:100 rabbit polyclonal), anti-DsRed fluorescent protein/mCherry (1:50 rabbit polyclonal, Clontech, Mountain View, CA), anti-HA (1:200 mouse monoclonal, Roche Diagnostics), anti-phosphorylated H2A/H2A.X (1:200 rabbit polyclonal 07-745, Upstate Biotechnology, Charlottesville, VA) and anti-phosphorylated H2A.X (1:200 mouse monoclonal, BioLegend, San Diego, CA).

Proximity ligation assay

To test if two proteins occupy adjacent positions within the cell, we applied a proximity ligation assay [32]. Conventional cell preparations were first incubated with primary antibodies generated in the rabbit and in the mouse, respectively, which recognize the proteins of interest. Next, secondary anti-rabbit and anti-mouse antibodies coupled with short complementing DNA strands (Olink Bioscience, Uppsala, SWE) were applied, using the immunostaining protocol from above. Reactions for the ligation of DNA strands to a circularized oligo and the subsequent rolling circle amplification incorporating labeled nucleotides were performed using the Duolink II kit (Olink Bioscience, Uppsala, SWE) according to the instructions of the manufacturer. Slides were washed and mounted under a coverslip in Vectashield plus DAPI as above. Fluorescence indicating the interaction between oligonucleotides attached to neighboring antigens was evaluated under the fluorescence microscope.

Fluorescent in situ hybridization (FISH)

Cells from 5 ml of conjugating cell suspension were pelleted and fixed in 1 ml of Carnoy's fixative (methanol-chloroform-acetic acid, 6:3:2). After 1 h at room temperature, cells were pelleted and resuspended in 500 µl of 70% ethanol. A few drops of this suspension were applied to a slide and air-dried. A FISH probe was produced by pooling PCR-amplified sequences corresponding to a 22.1 kb intercalary chromosomal region [29]. The purified PCR products were labeled with Cy3 by nick translation. The probe and chromosomal DNA were denatured by hot formamide and hybridized for 36 h at 37°C.

Microscopy and documentation

Fluorescent signals generated by DAPI, immunostaining, proximity ligation or FISH were visualized by appropriate filter combinations in a fluorescence microscope and recorded with a cooled CCD camera. Of thick DAPI- and immuno-stained nuclei, z stacks were taken using MetaView software (Universal Imaging, Downingtown, PA), deconvolved using AutoDeblur (AutoQuant Imaging, Watervliet, NY) and projected with ImageJ (Wayne Rasband, N.I.H.; http://rsb.info.nih.gov/ij/) software. Images from different color channels were colorized and merged using Photoshop software.

For counting recombination foci and for colocalizing Dmc1p and γ-H2A.X signals in spread cells, image stacks were taken at 100× magnification and projected. In Photoshop, resolution was enhanced to 150 pixel/inch and brightness and contrast were adjusted to give optimal differentiation from background staining. A dot was counted as a recombination focus if its size and/or brightness was higher than the average background signal. Stretched foci were counted as single if they were oval or as two or more if they had constrictions. In all cases, the fluorescence was Cy3. For evaluating Dmc1-mCherry × *rad51*i and Dmc1-mCherry × wild type mating cells, the mCherry tag was enhanced with anti-dsRed and Cy3-coupled secondary antibody. For meioses of wild type × wild type matings, Dmc1p was detected using anti-Rad51/Dmc1 antiserum and Cy3-coupled secondary antibody.

To determine the brightness of fluorescence foci, gray values (within a range from 0–255) were measured on 8-bit images using ImageJ. For this, images of stained nuclei were adjusted to the same level of background signal intensity and the mean gray values of foci within a mask were calculated for the strongest ten foci for each evaluated nucleus.

Evaluation of colocalizing Dmc1p and γ-H2A.X signals was done on well-spread and flat regions of nuclei.

Supporting Information

Figure S1 Testing the efficiency of *rad51* RNAi. Expression of Rad51p was compared on Western blots from wild-type and from Rad51p-depleted (*rad51*i) strains. The Gel Analysis Tool of ImageJ (Wayne Rasband, N.I.H.; http://rsb.info.nih.gov/ij/) was used for measuring intensities of bands produced by the Rad51/Dmc1 antibody in Western blots such as the one shown in Figure 1C. The Dmc1p band served as an internal control. In three different *rad51*i lines, reductions to 7%, 3% and 1.14% of the wild-type level were found. In addition to estimating protein levels in cell samples, we determined Rad51p expression in individual cells: (A) Examples of vegetatively growing cells with the somatic nucleus displaying Rad51p spots (red). They are found in a majority of vegetatively growing wild-type cells (Loidl and Scherthan, J. Cell Sci 117: 5791–5801, 2004) and are missing in *rad51*i strains (data not shown). However, the lack of Rad51p spots is an unreliable indicator of RNAi efficiency since their presence and intensity is variable and they are altogether absent from ~20% of wild-type somatic nuclei (Loidl and Scherthan, J. Cell Sci 117: 5791–5801, 2004). Therefore, to estimate the efficiency of RNAi, we enforced expression of Rad51p in somatic nuclei by UV-irradiation and determined its reduction in the *rad51*i strain. (B) Starving *rad51*i cells and cells of a wildtype-like control strain (carrying a cellular GFP-marker - green) were mixed and exposed to 20 J/m² of short-wave UV to induce DNA damage (Loidl and Mochizuki, Mol Biol Cell 20: 2428–2437, 2009). The cells were fixed 90 min after UV

exposure, and damage-induced Rad51p expression in the somatic nuclei was detected by immunostaining with an antibody against Rad51p/Dmc1p (red). As can be seen, *rad51*i cells (as recognized by absence of the green marker protein) are unable to express Rad51p. In quantitative terms, in only 0.7% of *rad51*i cells (n = 1000), the somatic nucleus displayed Rad51p staining, whereas UV induced strong Rad51p staining in 100% (n = 300) of wild-type cells. (C) Western detection of Rad51p. In starving (as well as in vegetatively growing - data not shown) wild-type (WT) cells, Rad51p is expressed at a basal level. This expression was considerably increased upon treatment with UV whereas Rad51p expression was induced only weakly by UV in *rad51*i cells. (The lower row shows tubulin as a loading control.) Altogether, *rad51* RNAi can be considered as highly efficient.
Found at: doi:10.1371/journal.pgen.1001359.s001 (0.05 MB PDF)

Figure S2 The presence of the *RAD51* RNAi construct reduces chromosome compaction but does not adversely affect meiotic divisions. Two strains of different mating types, one containing the *RAD51* RNAi hairpin construct, the other wild-type, were starved in the absence of $CdCl_2$ and mixed to induce meiosis. In the absence of $CdCl_2$, dsRNA is not (or only weakly) transcribed and Rad51p is expressed. Meiotic nuclear elongation appeared normal in both partners (A) but entry into metaphase I was usually delayed in one partner (B - cell at the bottom). Also, bivalents in one partner were distinct entities (C - cell at top), whereas in the other they always appeared less condensed (C - cell at the bottom). Importantly however, metaphases I of neither partner showed signs of chromosome fragmentation. Meiotic divisions were slightly asynchronous: (D) shows one partner with the second meiotic division completed (top) and the other during anaphase II (bottom). By the end of meiosis, however, both the wild-type and the *rad51*hp cell displayed four meiotic products (E). This control experiment demonstrates that, while *rad51*hp cells displayed slight anomalies in chromosome condensation, the meiotic phenotypes of chromosome fragmentation and disturbed divisions seen in the presence of $CdCl_2$ are due to the depletion of Rad51p and not a side-effect of the presence of the construct. Additional indication against an adverse effect of the RNAi construct on meiosis comes from the observation that in the absence of $CdCl_2$, 60% of *rad51*hp matings produced viable sexual progeny (Table 1). This is slightly less than wild-type, but the difference can be accounted for by a residual RNAi effect in the absence of induction. Finally, $CdCl_2$ as such was excluded as the cause of aberrant meioses because it did not affect meiosis in a wild-type control. Bar: 10 μm.
Found at: doi:10.1371/journal.pgen.1001359.s002 (0.16 MB PDF)

Figure S3 Specificity of the anti-Rad51 antibody. While the anti-Rad51 antibody did not work on Western blots, there are two independent pieces of evidence that it is specific for Rad51p. (A) Pairwise stainings revealed that the anti-Rad51/Dmc1 antibody, the anti-Rad51 antibody, and HA-tagging of Rad51p all highlight

the same structures in somatic nuclei. (B) In cells where Rad51p is depleted by RNAi (for the efficiency of RNAi see Figure 1C), the antibody does not produce any signals. Here, a culture containing conjugating and non-conjugating cells was exposed to UV radiation (20 J/m^2) to strongly induce Rad51p expression. The conjugating cells to the left do not display Rad51p immunostaining because one of the two partners carries the *rad51*hp construct whose cadmium-induced transcription is sufficient to deplete both partners of Rad51p. The non-meiotic wild-type (WT) cell to the right expresses Rad51p in the somatic nucleus and serves as a control for functioning immunostaining.
Found at: doi:10.1371/journal.pgen.1001359.s003 (0.11 MB PDF)

Figure S4 Time course of meiotic stages in the wild type. Staging was performed by morphological criteria according to Sugai and Hiwatashi (J. Protozool. 21: 542–548, 1974), where I-IV indicate stages of increasing length of the meiotic nucleus, with maximal elongation at stage IV. Stage V corresponds to diplotene, and stage VI to diakinesis-metaphase I. For each timepoint, 200 nuclei were evaluated.
Found at: doi:10.1371/journal.pgen.1001359.s004 (0.04 MB PDF)

Figure S5 Principle of the proximity ligation assay. Preparations are first incubated with antibodies against the two proteins or tags generated in rabbit and mouse, respectively. Next, secondary anti-rabbit and anti-mouse antibodies coupled with short complementing DNA strands are applied. DNA strands are then ligated and polymerize by a rolling circle amplification, incorporating labeled nucleotides. This leads to a strong amplification of a microscopically detectable signal if the primary antibodies bind to one and the same protein or protein tag or to different but adjoining proteins or tags. Thus, the proximity ligation assay can be used for sensitivity enhancement or for testing if two proteins in question occupy adjacent positions within the cell (Söderberg et al., Nature Meth 3: 995–1000, 2006). See also the instructions of the manufacturer of the Duolink II kit (Olink Bioscience, Uppsala, SWE).
Found at: doi:10.1371/journal.pgen.1001359.s005 (0.07 MB PDF)

Figure S6 Estimation of the relative abundance of DSBs in the different genotypes at different time points.
Found at: doi:10.1371/journal.pgen.1001359.s006 (0.34 MB PDF)

Acknowledgments

Author Contributions

Conceived and designed the experiments: RAHT JL. Performed the experiments: RAHT AL JL. Analyzed the data: RAHT AL JL. Contributed reagents/materials/analysis tools: AL. Wrote the paper: RAHT JL.

References

1. Neale MJ, Keeney S (2006) Clarifying the mechanics of DNA strand exchange in meiotic recombination. Nature 442: 153–158.
2. Schwacha A, Kleckner N (1997) Interhomolog bias during meiotic recombination: meiotic functions promote a highly differentiated interhomolog-only pathway. Cell 90: 1123–1135.
3. Niu H, Wan L, Busygina V, Kwon Y, Allen JA, et al. (2009) Regulation of meiotic recombination via Mek1-mediated Rad54 phosphorylation. Mol Cell 36: 393–404.
4. Bishop DK, Park D, Xu L, Kleckner N (1992) *DMC1*: a meiosis-specific yeast homolog of *E. coli recA* required for recombination, synaptonemal complex formation, and cell cycle progression. Cell 69: 439–456.
5. Tsubouchi H, Roeder GS (2006) Budding yeast Hed1 down-regulates the mitotic recombination machinery when meiotic recombination is impaired. Genes Dev 20: 1766–1775.
6. Henry JM, Camahort R, Rice DA, Florens L, Swanson SK, et al. (2006) Mnd1/Hop2 facilitates Dmc1-dependent interhomolog crossover formation in meiosis of budding yeast. Mol Cell Biol 26: 2913–2923.
7. Sheridan S, Bishop DK (2006) Red-Hed regulation: recombinase Rad51, though capable of playing the leading role, may be relegated to supporting Dmc1 in budding yeast meiosis. Genes Dev 20: 1685–1691.
8. Pittman DL, Cobb J, Schimenti KJ, Wilson LA, Cooper DM, et al. (1998) Meiotic prophase arrest with failure of chromosome synapsis in mice deficient for Dmc1, a germline-specific RecA homolog. Mol Cell 1: 697–705.
9. Yoshida K, Kondoh G, Matsuda Y, Habu T, Nishimune Y, et al. (1998) The mouse RecA-like gene Dmc1 is required for homologous chromosome synapsis during meiosis. Mol Cell 1: 707–718.

10. Couteau F, Belzile F, Horlow C, Grandjean O, Vezon D, et al. (1999) Random chromosome segregation without meiotic arrest in both male and female meiocytes of a *dmc1* mutant of *Arabidopsis*. Plant Cell 11: 1623–1634.

11. Siaud N, Dray E, Gy I, Gerard E, Takvorian N, et al. (2004) Brca2 is involved in meiosis in *Arabidopsis thaliana* as suggested by its interaction with Dmc1. EMBO J 23: 1392–1401.

12. Grishchuk AL, Kohli J (2003) Five RecA-like proteins of *Schizosaccharomyces pombe* are involved in meiotic recombination. Genetics 165: 1031–1043.

13. Lukaszewicz A, Howard-Till RA, Novatchkova M, Mochizuki K, Loidl J (2010) *MRE11* and *COM1/SAE2* are required for double-strand break repair and efficient chromosome pairing during meiosis of the protist *Tetrahymena*. Chromosoma 119: 505–518.

14. Eisen JA, Coyne RS, Wu M, Wu D, Thiagarajan M, et al. (2006) Macronuclear genome sequence of the ciliate *Tetrahymena thermophila*, a model eukaryote. PLoS Biol 4: e286. doi:10.1371/journal.pbio.0040286.

15. Marsh TC, Cole ES, Stuart KR, Campbell C, Romero DP (2000) *RAD51* is required for propagation of the germinal nucleus in *Tetrahymena thermophila*. Genetics 154: 1587–1596.

16. Campbell C, Romero DP (1998) Identification and characterization of the RAD51 gene from the ciliate *Tetrahymena thermophila*. Nucleic Acids Res 26: 3165–3172.

17. Smith JJ, Cole ES, Romero DP (2004) Transcriptional control of RAD51 expression in the ciliate *Tetrahymena thermophila*. Nucleic Acids Res 32: 4313–4321.

18. Loidl J, Scherthan H (2004) Organization and pairing of meiotic chromosomes in the ciliate *Tetrahymena thermophila*. J Cell Sci 117: 5791–5801.

19. Miao W, Xiong J, Bowen J, Wang W, Liu Y, et al. (2009) Microarray analyses of gene expression during the *Tetrahymena thermophila* life cycle. PLoS ONE 4: e4429. doi:10.1371/journal.pone.0004429.

20. Howard-Till RA, Yao MC (2006) Induction of gene silencing by hairpin RNA expression in *Tetrahymena thermophila* reveals a second small RNA pathway. Mol Cell Biol 26: 8731–8742.

21. Collins K, Gorovsky MA (2005) *Tetrahymena thermophila*. Curr Biol 15: R17–R18.

22. Cole ES, Cassidy-Hanley D, Hemish J, Tuan J, Bruns PJ (1997) A mutational analysis of conjugation in *Tetrahymena thermophila*. 1. Phenotypes affecting early development: meiosis to nuclear selection. Dev Biol 189: 215–232.

23. Westmoreland J, Ma WJ, Yan Y, Van Hulle K, Malkova A, et al. (2009) RAD50 is required for efficient initiation of resection and recombinational repair at random, γ-induced double-strand break ends. PLoS Genet 5: e1000656. doi:10.1371/journal.pgen.1000656.

24. Dickey JS, Redon CE, Nakamura AJ, Baird BJ, Sedelnikova OA, et al. (2009) H2AX: functional roles and potential applications. Chromosoma 118: 683–692.

25. Mochizuki K, Novatchkova M, Loidl J (2008) DNA double-strand breaks, but not crossovers, are required for the reorganization of meiotic nuclei in *Tetrahymena*. J Cell Sci 121: 2148–2158.

26. Song XY, Gjoneska E, Ren QH, Taverna SD, Allis CD, et al. (2007) Phosphorylation of the SQ H2A.X motif is required for proper meiosis and mitosis in *Tetrahymena thermophila*. Mol Cell Biol 27: 2648–2660.

27. Peoples-Holst TL, Burgess SM (2005) Multiple branches of the meiotic recombination pathway contribute independently to homolog pairing and stable juxtaposition during meiosis in budding yeast. Genes Dev 19: 863–874.

28. Zickler D (2006) From early homologue recognition to synaptonemal complex formation. Chromosoma 115: 158–174.

29. Loidl J, Mochizuki K (2009) *Tetrahymena* meiotic nuclear reorganization is induced by a checkpoint kinase-dependent response to DNA damage. Mol Biol Cell 20: 2428–2437.

30. Shinohara A, Shinohara M (2004) Roles of RecA homologues Rad51 and Dmc1 during meiotic recombination. Cytogenet Genome Res 107: 201–207.

31. Ivanov EL, Sugawara N, Fishman-Lobell J, Haber JE (1996) Genetic requirements for the single-strand annealing pathway of double-strand break repair in *Saccharomyces cerevisiae*. Genetics 142: 693–704.

32. Söderberg O, Gullberg M, Jarvius M, Ridderstråle K, Leuchowius K-J, et al. (2006) Direct observation of individual endogenous protein complexes *in situ* by proximity ligation. Nature Meth 3: 995–1000.

33. San Filippo J, Sung P, Klein H (2008) Mechanism of eukaryotic homologous recombination. Annu Rev Biochem 77: 229–257.

34. Sheridan SD, Yu X, Roth R, Heuser JE, Sehorn MG, et al. (2008) A comparative analysis of Dmc1 and Rad51 nucleoprotein filaments. Nucl Acids Res 36: 4057–4066.

35. Shinohara M, Gasior SL, Bishop DK, Shinohara A (2000) Tid1/Rdh54 promotes colocalization of Rad51 and Dmc1 during meiotic recombination. Proc Natl Acad Sci USA 97: 10814–10819.

36. Shinohara A, Gasior S, Ogawa T, Kleckner N, Bishop DK (1997) *Saccharomyces cerevisiae* recA homologues *RAD51* and *DMC1* have both distinct and overlapping roles in meiotic recombination. Genes Cells 2: 615–629.

37. Vignard J, Siwiec T, Chelysheva L, Vrielynck N, Gonord F, et al. (2007) The interplay of RecA-related proteins and the MND1-HOP2 complex during meiosis in *Arabidopsis thaliana*. PLoS Genet 3: e176. doi:10.1371/journal.pgen.0030176.

38. Bishop DK (1994) RecA homologs Dmc1 and Rad51 interact to form multiple nuclear complexes prior to meiotic chromosome synapsis. Cell 79: 1081–1092.

39. Thompson DA, Stahl FW (1999) Genetic control of recombination partner preference in yeast meiosis: isolation and characterization of mutants elevated for meiotic unequal sister-chromatid recombination. Genetics 153: 621–641.

40. Mancera E, Bourgon R, Brozzi A, Huber W, Steinmetz LM (2008) High-resolution mapping of meiotic crossovers and non-crossovers in yeast. Nature 454: 479–485.

41. Ashley T, Plug AW, Xu J, Solari AJ, Reddy G, et al. (1995) Dynamic changes in Rad51 distribution on chromatin during meiosis in male and female vertebrates. Chromosoma 104: 19–28.

42. Franklin AE, McElver J, Sunjevaric I, Rothstein R, Bowen B, et al. (1999) Three-dimensional microscopy of the Rad51 recombination protein during meiotic prophase. Plant Cell 11: 809–824.

43. Terasawa M, Shinohara A, Hotta Y, Ogawa H, Ogawa T (1995) Localization of RecA-like recombination proteins on chromosomes of the lily at various meiotic stages. Genes Dev 9: 925–934.

44. Niu H, Wan L, Baumgartner B, Schaefer D, Loidl J, et al. (2005) Partner choice during meiosis is regulated by Hop1-promoted dimerization of Mek1. Mol Biol Cell 16: 5804–5818.

45. Carballo JA, Johnson AL, Sedgwick SG, Cha RS (2008) Phosphorylation of the axial element protein Hop1 by Mec1/Tel1 ensures meiotic interhomolog recombination. Cell 132: 758–770.

46. Lin FM, Lai YJ, Shen HJ, Cheng YH, Wang TF (2010) Yeast axial-element protein, Red1, binds SUMO chains to promote meiotic interhomologue recombination and chromosome synapsis. EMBO J 29: 586–596.

47. Goldfarb T, Lichten M (2010) Frequent and efficient use of the sister chromatid for DNA double-strand break repair during budding yeast meiosis. PLoS Biol 8: e1000520. doi:10.1371/journal.pbio.1000520.

48. Latypov V, Rothenberg M, Lorenz A, Octobre G, Csutak O, et al. (2010) Roles of Hop1 and Mek1 in meiotic chromosome pairing and recombination partner choice in *Schizosaccharomyces pombe*. Mol Cell Biol 30: 1570–1581.

49. Couteau F, Nabeshima K, Villeneuve A, Zetka M (2004) A component of *C. elegans* meiotic chromosome axes at the interface of homolog alignment, synapsis, nuclear reorganization, and recombination. Curr Biol 14: 585–592.

50. Orias E, Hamilton EP, Orias JD (2000) *Tetrahymena* as a laboratory organism: useful strains, cell culture, and cell line maintenance. In: Asai DJ, Forney JD, eds. Tetrahymena thermophila. San Diego: Academic Press. pp 189–211.

51. Mochizuki K (2008) High efficiency transformation of *Tetrahymena* using a codon-optimized neomycin resistance gene. Gene 425: 79–83.

52. Bruns P, Cassidy-Hanley D (2000) Biolistic transformation of macro- and micronuclei. Methods Cell Biol 62: 501–512.

53. Shang Y, Song X, Bowen J, Corstanje R, Gao Y, et al. (2002) A robust inducible-repressible promoter greatly facilitates gene knockouts, conditional expression, and overexpression of homologous and heterologous genes in *Tetrahymena thermophila*. Proc Natl Acad Sci USA 99: 3734–3739.

54. Yao MC, Yao CH (1989) Accurate processing and amplification of cloned germ line copies of ribosomal DNA injected into developing nuclei of *Tetrahymena thermophila*. Mol Cell Biol 9: 1092–1099.

55. Martindale DW, Allis CD, Bruns PJ (1982) Conjugation in *Tetrahymena thermophila*. A temporal analysis of cytological stages. Exp Cell Res 140: 227–236.

56. Karrer KM (2000) *Tetrahymena* genetics: two nuclei are better than one. In: Asai DJ, Forney JD, eds. Tetrahymena thermophila. San Diego: Academic Press. pp 127–186.